

Instabilities of steps induced by the drift of adatoms and effect of the step permeability

メタデータ	言語: eng 出版者: 公開日: 2017-10-05 キーワード (Ja): キーワード (En): 作成者: メールアドレス: 所属:
URL	https://doi.org/10.24517/00028538

This work is licensed under a Creative Commons Attribution-NonCommercial-ShareAlike 3.0 International License.



Instabilities of steps induced by the drift of adatoms and effect of the step permeability

Masahide Sato,^{1,2} Makio Uwaha,¹ and Yukio Saito³

¹*Department of Physics, Nagoya University, Furo-cho, Chikusa-ku, Nagoya 464-8602, Japan*

²*Computer Center, Gakushuin University, 1-5-1 Mejiro, Toshima-ku, Tokyo 171-8588, Japan*

³*Department of Physics, Keio University, 3-14-1 Hiyoshi, Kohoku-ku, Yokohama 223-8522, Japan*

(Received 25 April 2000)

We theoretically study step wandering and step bunching induced by the drift of adatoms with attention to the permeability of steps. The critical drift velocity to induce the instability is calculated, and Monte Carlo simulation is performed to test the linear analysis. In sublimation, when the step distance is small in comparison with the surface diffusion length, the wandering and bunching of steps can occur simultaneously with the step-down drift if steps are impermeable. The instabilities do not occur simultaneously if steps are permeable: the bunching occurs with the step-up drift, and the wandering with the step-down drift. In growth, when the step distance is small, the bunching occurs with the step-down drift and the step wandering occurs with the step-up drift irrespective of the permeability, in agreement with Métois and Stoyanov [Surf. Sci. **440**, 407 (1999)]. The change of the permeability with increasing temperature can explain the instabilities observed in Si(111) vicinal face [M. Degawa *et al.*, Jpn. J. Appl. Phys. **38**, L308 (1999)].

I. INTRODUCTION

Step bunching in a vicinal face of Si(111) in sublimation by heating with direct electric current has been a long standing mystery because the current direction to induce the bunching changes several times as temperature changes.¹⁻⁷ According to Homma and Aizawa⁷ the bunching occurs with step-down current in the lowest temperature range (range I: 860 °C < T < 960 °C) and the third temperature range (range III: 1210 °C < T < 1300 °C) while it occurs with step-up current in the second (range II: 1060 °C < T < 1190 °C) and the fourth (range IV: 1320 °C < T) temperature ranges. The heating current induces drift of adsorbed atoms (adatoms) either parallel or antiparallel to the external electric field according to the effective charge of an adatom. The cause of the change has been attributed to the change of the effective charge,⁸ to the change of diffusion length^{9,10} and to the diffusion of surface vacancies.¹¹ Recently Stoyanov proposed a different mechanism, that is the change of permeability of steps.¹² Step bunching was also observed during growth in ranges I-III. In all these temperature ranges the bunching always occurs with the step-down current¹³ (no experiment was performed in range IV): the current direction for bunching is reversed in range II compared with the sublimation case. As explained by Métois and Stoyanov, the reversal is consistent to the interpretation that the steps are permeable in range II.

If the kink density along the step is high, an adatom attaching to the step always reaches a kink position to solidify. The adatoms crossing the step without solidification are negligibly few, and the step is called impermeable (nontransparent). In the impermeable case, the step bunching was studied theoretically with a step flow model.^{9,10,14-22} When the distance between steps is smaller than the surface diffusion length, which situation is likely for a Si(111) vicinal face,^{2,3} the step bunching is possible with the step-down drift in sublimation. There is a critical drift velocity above which the bunching occurs, and it is determined by the strength of the repulsive interaction between steps.^{10,15,16,20-22} If the step is impermeable in ranges I, II, and III, the reversal of the cur-

rent direction may be explained by the change of the effective charge Z_{eff} :⁸ a positive charge in ranges I and III, and a negative charge in range II (we do not consider range IV in this paper). In the bunching, the size of a bunch (or equivalently the width of the large terrace) increases with the annealing time in a power law $L \sim t^\beta$.⁵ The theoretical value $\beta = 1/2$ (Refs. 18, 20, and 21) agrees with the experiment. However, in a recent experiment²³ the observation of the surface profile of a grooved surface after heating with current suggests that the drift direction is always parallel to the current irrespective of temperature.

Theoretically in a vicinal face two kinds of instabilities, step bunching and step wandering,^{22,24,25} are possible. Recently Degawa *et al.* observed both bunching and the wandering by using a cylindrical specimen.²⁶ At 1000 °C (in range II), in-phase wandering occurs with the step-down current, while bunching occurs with a step-up current. Although a step wandering instability with the drift of adatoms has been predicted, the current direction to induce the wandering is the same as the bunching instability if steps are impermeable. Therefore, the instabilities cannot be explained simply by the change of the effective charge.

If the kink density along the step is low, adatoms attaching to a straight part of the step may not reach a kink position and leave the step without solidification. The adatoms crossing the step without solidification are not negligible, and the step is called permeable (transparent). Stoyanov studied the stability of an isolated bunch consisting of permeable steps in the drift flow, and found that the isolated bunch is stable with the step-up drift.¹² Therefore, without a change of sign of the effective charge, a reversal of the current direction for bunching is possible from a change of the step permeability: the steps are impermeable in ranges I and III, and permeable in range II. The relation between the step distance and the number of steps in a bunch,²⁷ as well as the observed bunching in growth,¹³ support this interpretation. Then if theory predicts the wandering instability of permeable steps with step-down drift in sublimation, the above interpretation is consistent with the observation of wandering instability.

In this paper, we study the instabilities of permeable and impermeable steps both in growth and in sublimation. By a linear analysis we derive quantitative conditions for the instabilities to occur. Then we carry out a Monte Carlo simulation to test the theory, at least qualitatively.

II. MODEL

A. Continuum model for a mathematical analysis

We use the standard step flow model with drift of adatoms^{9,10,14–22,24,25} for a mathematical analysis of the step motion. When the drift is perpendicular to the average orientation of steps, the diffusion equation of the adatom density $c(\mathbf{r}, t)$, on a terrace, is given by

$$\frac{\partial c}{\partial t} = D_s \nabla^2 c - v \frac{\partial c}{\partial y} - \frac{1}{\tau} c + F, \quad (2.1)$$

where D_s is the diffusion constant, τ the adatom lifetime for evaporation, v the drift velocity (which can be written as $v = Z_{\text{eff}} e E D_s / k_B T$ with the applied electric field E), and F the impingement rate of atoms. We suppose that the steps are parallel to the x axis on average, and that the y axis points toward the step-down direction. Unless the adatom density is very high and the step motion is fast, we may use the quasi-static approximation for the diffusion equation (2.1):

$$D_s \nabla^2 c - v \frac{\partial c}{\partial y} - \frac{1}{\tau} c + F = 0. \quad (2.2)$$

The adatom current is given by

$$\mathbf{j}(\mathbf{r}) = -D_s \nabla c(\mathbf{r}) + v c(\mathbf{r}) \mathbf{e}_y, \quad (2.3)$$

where the first term is due to the surface diffusion and the second term is due to the drift of adatoms. The terrace is bounded by steps, where solidification and melting occur. We may consider that some adatoms solidify at the step position, and others cross over the step to the neighboring terraces without solidification. Then the boundary conditions at the steps are given by^{18,28} the growth current

$$\begin{aligned} K_+(c|_{\zeta_{m+}} - c_m) &= \hat{\mathbf{n}} \cdot (D_s \nabla c|_{\zeta_{m+}} - v \mathbf{e}_y c|_{\zeta_{m+}}) \\ &= K_+(c|_{\zeta_{m+}} - c_m) + P(c|_{\zeta_{m+}} - c|_{\zeta_{m-}}), \end{aligned} \quad (2.4)$$

$$\begin{aligned} K_-(c|_{\zeta_{m-}} - c_m) &= -\hat{\mathbf{n}} \cdot (D_s \nabla c|_{\zeta_{m-}} - v \mathbf{e}_y c|_{\zeta_{m-}}) \\ &= K_-(c|_{\zeta_{m-}} - c_m) + P(c|_{\zeta_{m-}} - c|_{\zeta_{m+}}), \end{aligned} \quad (2.5)$$

where $\hat{\mathbf{n}}$ is the unit vector normal to the step in the step-down direction, $y = \zeta_m(x, t)$ the position of the m th step, $K_{+(-)}$ the kinetic coefficient, and P the permeability coefficient of the step. The subscript $+(-)$ indicates the lower (upper) side of the step. The equivalent electric circuit for an isolated step (without external field) is shown in Fig. 1(a). The rate of the adatoms permeating the step is proportional to the difference of the adatom densities in the lower and upper sides of the step. The solidification rate is proportional to the difference of the adatom density at the step and that in equilibrium. The equilibrium adatom density is given by

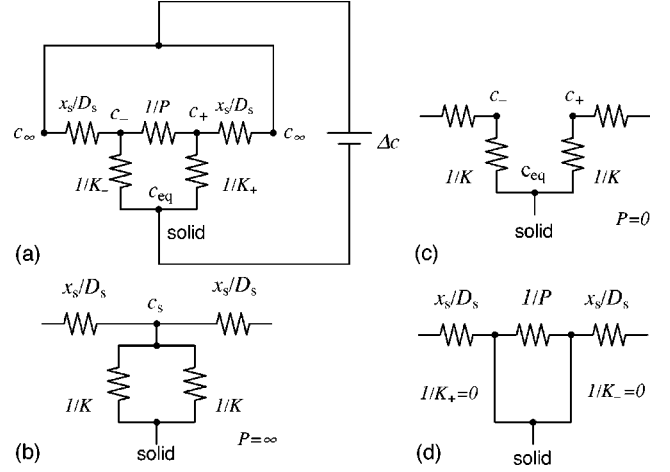


FIG. 1. Electric circuits equivalent to a single step in the super-saturated adatom density c_∞ . The resistance is defined by $R = \Delta c / j$, where j is the atomic current. (a) With general boundary condition. (b) For a perfectly permeable step. (c) For an impermeable step. (d) In the limit of fast step kinetics.

$$c_m(x) = c_{\text{eq}}^0 \left(1 - \frac{\Omega f_m(x)}{k_B T} \right), \quad (2.6)$$

where c_{eq}^0 is the equilibrium adatom density for a straight step, and $f_m(x)$ the force acting on the m th step. When we take account of the step tension and the interaction between steps, the force f_m is given by

$$f_m = -\tilde{\beta} \kappa_m - \frac{\partial \xi_m}{\partial \zeta_m}, \quad (2.7)$$

where κ_m is the curvature of the m th step, $\tilde{\beta}$ the step stiffness, and ξ_m the step energy. [Equation (2.6) is an approximation and the general form is given in Ref. 29.] With a step energy ξ_m of the form

$$\xi_m(x) = \xi_0 + \sum_{n=m \pm 1} U[|\zeta_m(x) - \zeta_n(x)|], \quad (2.8)$$

the equilibrium adatom density c_m becomes

$$\begin{aligned} c_m(x) &= c_{\text{eq}}^0 + \frac{\Omega c_{\text{eq}}^0 \tilde{\beta} \kappa_m(x)}{k_B T} \\ &+ \frac{\nu \Omega c_{\text{eq}}^0 A}{k_B T} \sum_{n=m \pm 1} \frac{1}{[\zeta_m(x) - \zeta_n(x)]^{\nu+1}}, \end{aligned} \quad (2.9)$$

where we use $U(l) = A/l^\nu$ as the repulsive interaction potential. In this paper we use $\nu = 2$ as the exponent of the repulsive interaction potential, which corresponds to the elastic interaction.³⁰ For simplicity, we will only study the perfectly permeable case $P \rightarrow \infty$ and the impermeable case, case $P = 0$, to clarify the effect of the step permeability.

B. Lattice model for simulation

To check the mathematical analysis we carry out Monte Carlo simulation. We consider a square lattice with periodic boundary conditions. The lattice constant and step height are $a = 1$. We use solid-on-solid (SOS) steps: overhanging of a

step is excluded and the step position is a single-valued function of x . Two-dimensional nucleation on terraces is forbidden. The algorithm of the simulation is similar to that of Refs. 31 and 32, except that the jump of adatoms over the step is allowed without an extra diffusion barrier to include the permeability of adatoms at step sites.^{25,33} The uniform drift of adatoms is taken into account as a biased diffusion probability. This treatment is valid when the adatom density is low. We choose the time increment for a diffusion trial $\Delta t = 1/4N_a$ (N_a is the number of adatoms) in order to make the diffusion constant $D_s = 1$. When the drift velocity is v , an adatom on the site (i, j) moves to the site $(i \pm 1, j)$ with the transition probability $1/4$, and to the site $(i, j \pm 1)$ with the probability $(1 \pm v/2)/4$ in a diffusion trial if the destination is empty. When an adatom comes in front of a step, the adatom solidifies with the probability

$$p_s = \left[1 + \exp\left(\frac{\Delta E_s + \Delta U - \phi}{k_B T}\right) \right]^{-1}. \quad (2.10)$$

The increment of the step energy by the solidification ΔE_s is given by $\Delta E_s = \epsilon \times$ (the increment of the step perimeter), where the nearest-neighbor bond energy ϵ is related to the step stiffness $\tilde{\beta}$ as

$$\frac{\tilde{\beta}}{k_B T} = \frac{(1 - e^{-\epsilon/k_B T})^2}{2e^{-\epsilon/k_B T}}. \quad (2.11)$$

The change of the step-step interaction potential ΔU , when the position of m th step $[i, \zeta_m(i)]$ moves to $[i, \zeta'_m(i)]$, is given by

$$\begin{aligned} \Delta U &= \sum_{n=m \pm 1} \{U[|\zeta'_m(i) - \zeta_n(i)|] - U[|\zeta_m(i) - \zeta_n(i)|]\} \\ &= A \sum_{n=m \pm 1} [|\zeta'_m(i) - \zeta_n(i)|^{-2} - |\zeta_m(i) - \zeta_n(i)|^{-2}]. \end{aligned} \quad (2.12)$$

The chemical potential gain by the solidification ϕ determines the equilibrium adatom density c_{eq}^0 as

$$c_{\text{eq}}^0 = \frac{1}{1 + e^{\phi/k_B T}}. \quad (2.13)$$

To satisfy the detailed balance, an atom in the step melts, and becomes an adatom with the probability

$$p_m = \left[1 + \exp\left(\frac{\Delta E_s + \Delta U + \phi}{k_B T}\right) \right]^{-1} \quad (2.14)$$

if there is not an adatom on top of the atom. To select an atom that does the transition trial, we prepare a single table for all atoms and step atoms and pick up one atom from the table. Then the kinetic coefficient $K_- + K_+ = 4$. This algorithm is for perfectly permeable steps. The algorithm for an impermeable step is introduced in Sec. IV A and in Appendix A.

III. WANDERING INSTABILITY OF THE PERMEABLE STEP

When a step is perfectly permeable, $P \rightarrow \infty$, the adatom densities in the upper and the lower side of the step are the same [see Fig. 1(b)]:

$$c|_s = c|_{\zeta_{m+}} = c|_{\zeta_{m-}}. \quad (3.1)$$

This is the boundary condition used in the original model of Burton, Cabrera, and Frank.³⁴ The step velocity to the normal direction V_n is given by

$$V_n = 2\Omega K(c_s - c_m) = \Omega D_s \hat{n} \cdot (\nabla c|_{\zeta_{m+}} - \nabla c|_{\zeta_{m-}}), \quad (3.2)$$

where Ω is the atomic area, and K is the average kinetic coefficient defined by $K = (K_+ + K_-)/2$. Solidifying atoms are supplied by the diffusion current from both terraces. Since there is no gap in the adatom density at the step, there is no contribution of the drift current to the step velocity. By solving Eq. (2.2) with the boundary conditions (3.1) and (3.2), the normal velocity V_n is determined. Time evolution of the step position $\zeta_m(x, t)$ is related to the normal velocity V_n as

$$\frac{\partial \zeta_m}{\partial t} = V_n \sqrt{1 + \left(\frac{\partial \zeta_m}{\partial x}\right)^2}. \quad (3.3)$$

A. Wandering of an isolated step

We first study the motion of an isolated step without impingement of atoms: $F = 0$. The boundary conditions far from the step are $c(y \rightarrow \pm \infty) = 0$, and the velocity of the straight step V_0 is calculated as

$$V_0 = -\frac{2D_s c_{\text{eq}}^0 \sqrt{\tilde{v}^2 + 4}}{x_s (2 + \lambda \sqrt{\tilde{v}^2 + 4})}, \quad (3.4)$$

where $x_s = \sqrt{D_s} \tau$ is the surface diffusion length, and the scaled quantities are defined as $\tilde{v} = vx_s/D_s$ and $\lambda = D_s/Kx_s$. With a sinusoidal perturbation of the wave number q to the straight step, the position of the step is given by $\zeta_1 = V_0 t + \delta \zeta e^{iqx + \omega_q t}$, where ω_q is the amplification rate in the linear theory. By solving the diffusion equation, we obtain the rate ω_q as

$$\begin{aligned} \omega_q x_s^2 &= \frac{2\tilde{v}(\sqrt{\tilde{v}^2 + 4 + 4\tilde{q}^2} - \sqrt{\tilde{v}^2 + 4})}{\Omega D_s c_{\text{eq}}^0 (2 + \lambda \sqrt{\tilde{v}^2 + 4})(2 + \lambda \sqrt{\tilde{v}^2 + 4 + 4\tilde{q}^2})} \\ &\quad - \frac{2\tilde{\Gamma} \tilde{q}^2 \sqrt{\tilde{v}^2 + 4 + 4\tilde{q}^2}}{(2 + \lambda \sqrt{\tilde{v}^2 + 4 + 4\tilde{q}^2})}, \end{aligned} \quad (3.5)$$

where $\tilde{q} = qx_s$ and $\tilde{\Gamma} = \Omega \tilde{\beta}/k_B T x_s$.

When the wavelength of the fluctuation is longer than the surface diffusion length $qx_s \ll 1$, the amplification rate ω_q is expressed as

$$\omega_q \approx \alpha_2 q^2 + \alpha_4 q^4 + \dots, \quad (3.6)$$

where

$$\frac{\alpha_2}{\Omega D_s c_{\text{eq}}^0} = \frac{2[2\tilde{v} - \tilde{\Gamma}(4 + \tilde{v}^2)(2 + \lambda\sqrt{4 + \tilde{v}^2})]}{(2 + \lambda\sqrt{4 + \tilde{v}^2})^2 \sqrt{4 + \tilde{v}^2}}, \quad (3.7)$$

$$\frac{\alpha_4}{\Omega D_s c_{\text{eq}}^0 x_s^2} = -\frac{2[\tilde{v}(2 + 3\lambda\sqrt{4 + \tilde{v}^2}) + \tilde{\Gamma}(4 + \tilde{v}^2)(2 + \lambda\sqrt{4 + \tilde{v}^2})]}{(2 + \lambda\sqrt{4 + \tilde{v}^2})^3 (4 + \tilde{v}^2)^{3/2}}. \quad (3.8)$$

The coefficient α_2 determines the stability at long wavelength. If \tilde{v} is small, \tilde{v}^2 is negligible, and

$$\frac{\alpha_2}{\Omega D_s c_{\text{eq}}^0} = \frac{1}{2(1 + \lambda)} \left[\frac{\tilde{v}}{(1 + \lambda)} - 4\tilde{\Gamma} \right], \quad (3.9)$$

which is the same as the corresponding coefficient for the impermeable step²⁴ when the step kinetics is fast, $\lambda \rightarrow 0$. The first term is the effect of the drift, which is destabilizing if $\tilde{v} > 0$, and the second term is the effect of the stiffness, which stabilizes a straight step. As a result of competition between these effects, the straight step is unstable with the step-down drift whose velocity exceeds the critical value,

$$v_c^W = \frac{4\Omega D_s \tilde{\beta}(1 + \lambda)}{k_B T x_s^2}. \quad (3.10)$$

For v larger than v_c^W , a small fluctuation grows exponentially. If we include thermal fluctuation in our model as a random force, the amplitude of the step fluctuation is determined by α_2 and $\langle \delta \zeta^2 \rangle \propto |\alpha_2|^{-1}$ for the stable case.^{31,32} (Near the critical point, nonlinearity becomes important.³⁵) Therefore, we expect the enhancement of fluctuation with $\tilde{v} > 0$ and suppression with $\tilde{v} < 0$. The coefficient α_4 determines the stability at short wavelength. When \tilde{v} is small, \tilde{v}^2 is negligible, and

$$\frac{\alpha_4}{\Omega D_s c_{\text{eq}}^0} = -\frac{1}{8(1 + \lambda)^2} \left[\frac{(1 + 3\lambda)\tilde{v}}{(1 + \lambda)} + 8\tilde{\Gamma} \right]. \quad (3.11)$$

For the wandering instability to occur the drift is in the step-down direction ($\tilde{v} > 0$), and α_4 is negative. The step is stable for the short wavelength fluctuation. The wavelength of the most unstable mode is determined as $\lambda_{\text{max}} = 2\pi\sqrt{2}|\alpha_4|/\alpha_2$, which becomes long near the threshold of the instability.

Since the amplitude of the fluctuation increases rapidly after the instability occurs, we need to take account of nonlinear effects to predict the step behavior. Since the wavelength of the most unstable mode is long near the threshold of the instability, the linear evolution equation is obtained from Eq. (3.6) by replacing ω_q and iq with $\partial/\partial t$ and $\partial/\partial x$. Higher order terms should reflect the inversion symmetry of the system in the x direction, $x \leftrightarrow -x$. Then the most dominant nonlinear term near the threshold of the instability is proportional to $(\partial\zeta/\partial x)^2$. This type of nonlinear term is related to the velocity increment of the inclined straight

step.^{25,36} The normal velocity of the inclined step $V_n(\zeta_x)$ is given by replacing \tilde{v}^2 with $\tilde{v}^2/(1 + \zeta_x^2)$ in Eq. (3.4). If we expand Eq. (3.3) as

$$\frac{\partial\zeta}{\partial t} = V_0 + \delta \left(\frac{\partial\zeta}{\partial x} \right)^2 + \dots, \quad (3.12)$$

the coefficient of the nonlinear term is given by

$$\delta = \frac{V_0}{2} + \frac{1}{2} \frac{d^2 V_n}{d\zeta_x^2} \approx \frac{V_0}{2} = -\frac{D_s c_{\text{eq}}^0}{x_s(1 + \lambda)}, \quad (3.13)$$

where we have neglected \tilde{v}^2 . Adding the nonlinear term to the linear equation, we obtain the nonlinear evolution equation

$$\frac{\partial\zeta}{\partial t} = -\alpha_2 \frac{\partial^2 \zeta}{\partial x^2} - \alpha_4 \frac{\partial^4 \zeta}{\partial x^4} + \delta \left(\frac{\partial\zeta}{\partial x} \right)^2. \quad (3.14)$$

This equation is called the Kuramoto-Sivashinsky equation,^{37,38} and its solution is known to produce spatiotemporal chaos. Therefore, near the threshold of the instability, the step is expected to show chaotic behavior if the anisotropy of crystal is negligible.^{24,25,32,39} The effect of the anisotropy is discussed in Refs. 40 and 41.

To confirm the above analysis we performed Monte Carlo simulation. Figure 2 represents the time evolution of an isolated step with the drift. The system size is 256×256 and the parameters are $\tau = 256$, $c_{\text{eq}}^0 = 0.18$ ($\phi/k_B T = 1.0$), and $\tilde{\beta}/k_B T = 0.54$ ($\epsilon/k_B T = 1.5$). The initial step position is $\zeta(x, t) = 0$. By using Eq. (3.7), the drift velocity to induce the wandering instability is estimated to be $8.8 \times 10^{-3} \leq v \leq 1.4$. Figure 2(a) shows the time evolution with the step-up drift ($v = -0.1$). The wandering fluctuation is suppressed and the receding step is more straight than that without the drift [Fig. 2(b)].²⁵ Figure 2(c) shows the time evolution with the step-down drift ($v = 0.1$). The drift velocity is in the unstable range and the wandering instability is evident. From Eq. (3.5) the wavelength of the most unstable mode is obtained as $\lambda_{\text{max}} \approx 36$, which agrees roughly with the period of the peaks of the wandering pattern observed in the initial stage of the instability. In the late stage the period of the peaks becomes longer. The positions of peaks are moving randomly along the step, and collision and creation of hills occur. The step pattern is similar to the chaotic pattern of a solution of Eq. (3.14) with negative δ .⁴²

B. Step wandering in a vicinal face

We consider a vicinal face consisting of equidistant parallel steps with a distance l . Wandering of the steps in the linear regime is expressed in terms of the position of the m th step as $\zeta_m = ml + \delta\zeta e^{iqx + imkl + \omega t}$. Since it is difficult to calculate ω for general q and k , we consider the simplest case: all steps fluctuate in phase, that is $k = 0$. When there is no impingement of the atoms, $F = 0$, the amplification rate ω is calculated in a similar way as in the isolated step case. It is given by

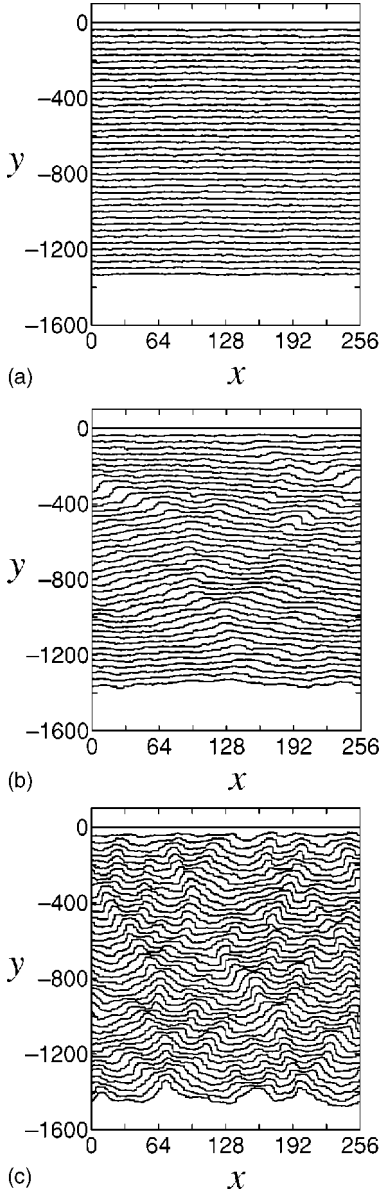


FIG. 2. Time evolution of the position of a perfectly permeable step in sublimation: (a) with the step-up drift ($v = -0.1$), (b) without the drift ($v = 0$), and (c) with the step-down drift ($v = 0.1$).

$$\begin{aligned}
\frac{\omega x_s^2}{\Omega c_{\text{eq}}^0 D_s} &= \frac{1}{\lambda g_0} \left(\tilde{v} \sinh \frac{\alpha \tilde{l}}{2} - \alpha \cosh \frac{\alpha \tilde{l}}{2} + \alpha e^{-\tilde{v} \tilde{l}/2} \right) \\
&- \frac{2}{\lambda g_0 g_q} \sinh \frac{\alpha_q \tilde{l}}{2} \left(\tilde{v} \sinh \frac{\alpha \tilde{l}}{2} - \alpha \cosh \frac{\alpha \tilde{l}}{2} \right. \\
&+ \left. \alpha e^{-\tilde{v} \tilde{l}/2} \right) - \frac{4 \alpha v}{g_0 g_q} \sinh \frac{\alpha_q \tilde{l}}{2} \left(\cosh \frac{\alpha \tilde{l}}{2} - \cosh \frac{\tilde{v} \tilde{l}}{2} \right) \\
&+ \frac{2 \alpha}{g_0 g_q} \left(\cosh \frac{\alpha \tilde{l}}{2} - \cosh \frac{\tilde{v} \tilde{l}}{2} \right) \\
&\times \left(\tilde{v} \sinh \frac{\alpha_q \tilde{l}}{2} + \alpha_q \cosh \frac{\alpha_q \tilde{l}}{2} - \alpha_q e^{-\tilde{v} \tilde{l}/2} \right) \\
&- \frac{\alpha_q}{g_q} \left(\cosh \frac{\alpha_q \tilde{l}}{2} - \cosh \frac{\tilde{v} \tilde{l}}{2} \right) \tilde{\Gamma} \tilde{q}^2, \quad (3.15)
\end{aligned}$$

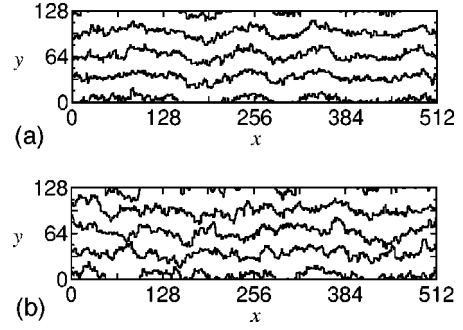


FIG. 3. Snapshots of the wandering of a train of perfectly permeable steps: (a) at $t = 4.1 \times 10^5$ with the repulsive interaction ($A/k_B T = 1000$), and (b) at $t = 4.1 \times 10^5$ without repulsive interaction. The drift is in the step-down direction ($v = 0.4$).

where

$$\tilde{l} = \frac{l}{x_s}, \quad (3.16)$$

$$\alpha = \sqrt{\tilde{v}^2 + 4}, \quad (3.17)$$

$$\alpha_q = \sqrt{\tilde{v}^2 + 4 + 4\tilde{q}^2}, \quad (3.18)$$

$$g_0 = 2\lambda \alpha \left(\cosh \frac{\alpha \tilde{l}}{2} - \cosh \frac{\tilde{v} \tilde{l}}{2} \right) + 2 \sinh \frac{\alpha \tilde{l}}{2}, \quad (3.19)$$

$$g_q = 2\lambda \alpha_q \left(\cosh \frac{\alpha_q \tilde{l}}{2} - \cosh \frac{\tilde{v} \tilde{l}}{2} \right) + 2 \sinh \frac{\alpha_q \tilde{l}}{2}. \quad (3.20)$$

When the step distance is smaller than the surface diffusion length, $l \ll x_s$, the amplification rate ω_q in the long-wavelength limit ($ql \ll 1$) is written as

$$\frac{\omega_q x_s^2}{\Omega D_s c_{\text{eq}}^0} \approx \left(\frac{\tilde{v} \tilde{l}^5}{360} - \tilde{\Gamma} \tilde{l} \right) \tilde{q}^2 + \dots, \quad (3.21)$$

which does not depend on the step kinetics λ . Similarly to the case of an isolated step [Eq (3.9)], the wandering instability is induced by the step-down drift. The critical drift velocity is

$$v_c^W = \frac{360 D_s \Omega \tilde{\beta} x_s^2}{k_B T l^4}, \quad (3.22)$$

which is larger than that of the isolated step. Since v_c^W is inversely proportional to $(l/x_s)^4$, the vicinal face rapidly becomes stable with decreasing step distance.

Figure 3 shows snapshots of the wandering instability of a step train. The system size is 512×128 and the number of steps is four. Initially the steps are straight with the same distance $l = 32$. The surface diffusion length is $x_s = 64$, which is twice as long as the initial step distance. The equilibrium adatom density is $c_{\text{eq}}^0 = 0.27$. To make the wandering instability accessible in the simulation, we use steps with small stiffness $\tilde{\beta}/k_B T = 0.13$. From Eq. (3.22) the critical drift velocity is estimated to $v_c^W = 0.18$. The strength of the repulsive interaction is $A = 1000$, with $\nu = 2$. Figure 3(a) rep-

resents the step wandering with the step-down drift ($v = 0.4$). By the repulsive interaction, the in-phase motion of the step wandering pattern is evident. When the repulsive interaction is turned off, although the in-phase mode has the largest growth mode, the phase coherence vanishes due to the randomness [Fig. 3(b)].

IV. WANDERING INSTABILITY OF IMPERMEABLE STEP

To study the wandering instability of impermeable steps, we need to change the boundary conditions [Eqs (3.1) and (3.2)]. Since the step is impermeable to the surface diffusion, adatoms cannot jump over the steps without solidification and the parameter for the permeability $P=0$ in Eqs. (2.4) and (2.5) [see Fig. 1(c)]. If the kinetic coefficient is finite, the gap of the adatom density is produced between the lower and upper sides of the step. Since the adatom flux to the step is proportional to the difference between the adatom density at the step and that at equilibrium, the boundary conditions are given by Eqs. (2.4) and (2.5) with $P=0$ (Refs. 9,10, and 14–16):

$$\begin{aligned} K_+(c|_{\xi_{m+}} - c_m) &= \hat{\mathbf{n}} \cdot (D_s \nabla c|_{\xi_{m+}} - v \mathbf{e}_y c|_{\xi_{m+}}) \\ &= K_+(c|_{\xi_{m+}} - c_m), \end{aligned} \quad (4.1)$$

$$\begin{aligned} K_-(c|_{\xi_{m-}} - c_m) &= \hat{\mathbf{n}} \cdot (-D_s \nabla c|_{\xi_{m-}} + v \mathbf{e}_y c|_{\xi_{m-}}) \\ &= K_-(c|_{\xi_{m-}} - c_m). \end{aligned} \quad (4.2)$$

The difference of the kinetic coefficients K_+ and K_- is the Ehrlich-Schwoebel (ES) effect,^{43,44} which can also induce the instabilities. If $K_+ > K_-$, the wandering instability occurs in growth^{32,39,45,46} and the bunching instability occurs in sublimation.^{44,47,48} For simplicity we neglect the ES effect and set $K_+ = K_- = K$. By solving the diffusion equation (2.2) with the boundary conditions [Eqs. (4.1) and (4.2)] we can calculate the profile of the adatom density. From the density profile the step velocity is determined by

$$\begin{aligned} V_n^m &= \Omega K_+(c|_{\xi_{m+}} - c_m) + \Omega K_-(c|_{\xi_{m-}} - c_m) \\ &= \Omega K(c|_{\xi_{m+}} + c|_{\xi_{m-}} - 2c_m). \end{aligned} \quad (4.3)$$

A. Wandering of an isolated step

We consider the wandering of an isolated step without the impingement of adatoms. By solving the diffusion equation with the boundary conditions far from the step ($c(y \rightarrow \pm \infty) = 0$), the velocity of the receding step is given by

$$V_0 = -\frac{\Omega D_s c_{\text{eq}}^0 (2\lambda + \alpha)}{x_s (1 + \lambda^2 + \alpha\lambda)}. \quad (4.4)$$

When we give a small perturbation $\zeta = \delta \zeta e^{iqx + \omega_q t}$ to the step, the amplification rate ω_q is calculated as

$$\begin{aligned} \frac{\omega_q x_s^2}{\Omega c_{\text{eq}}^0 D_s} &= \frac{(v - \alpha)(\alpha_q - \alpha)}{[\lambda(v + \alpha_q) + 2][\lambda(v + \alpha) + 2]} \\ &\quad + \frac{(v + \alpha)(\alpha_q - \alpha)}{[\lambda(v - \alpha_q) - 2][\lambda(v - \alpha) - 2]} \\ &\quad - \frac{\alpha_q + 2\lambda(1 + \tilde{q}^2)}{1 + \lambda^2(1 + \tilde{q}^2) + \alpha_q \lambda} \tilde{\Gamma} \tilde{q}^2. \end{aligned} \quad (4.5)$$

In the fast step kinetics limit, $\lambda \rightarrow 0$, Eq. (4.5) is simplified as

$$\begin{aligned} \frac{\omega_q x_s^2}{\Omega c_{\text{eq}}^0 D_s} &= \frac{\tilde{v}}{2} (\sqrt{\tilde{v}^2 + 4 + 4\tilde{q}^2} - \sqrt{\tilde{v}^2 + 4}) \\ &\quad - \tilde{\Gamma} \tilde{q}^2 \sqrt{\tilde{v}^2 + 4 + 4\tilde{q}^2}, \end{aligned} \quad (4.6)$$

which is, as expected, the same as the amplification rate of the permeable step [Eq. (3.5)] with $\lambda \rightarrow 0$. In this limit, since there is no kinetic barrier at the step, the gap in the adatom density disappears and we obtain eq. (3.1) [see Figs. 1(b) and 1(d)]. When the step kinetics is slow and $\lambda \gg 1$, the amplification rate ω_q is given by

$$\frac{\omega_q x_s^2}{\Omega c_{\text{eq}}^0 D_s} \approx \frac{3}{2\lambda^2} \left(\tilde{v} - \frac{4\lambda}{3} \tilde{\Gamma} \right) \tilde{q}^2 + \dots \quad (4.7)$$

for the long-wavelength fluctuation. The critical drift velocity is given by

$$v_c^W = \frac{4D_s^2 \Omega \tilde{\beta}}{3Kx_s^3 k_B T}. \quad (4.8)$$

Since v_c^W is inversely proportional to the kinetic coefficient K , with increasing the value of K , the critical drift velocity decreases and the step becomes less stable. Irrespective of the kinetics, a receding step becomes unstable with the step-down drift.

We carry out Monte Carlo simulation to test the linear stability analysis. The diffusion of the adatoms is the same as that for the permeable case except that the adatoms cannot jump over the steps [Fig. 4(a)]. When an adatom comes in front of a step site or just on the step site after a diffusion trial, the adatom tries to solidify [Fig. 4(b)]. The solidification of the adatom in front of the step is the same as that in the permeable case. On the other hand, the solidification of the adatom on the step site is tried only if the front of the site is not occupied by another adatom [Fig. 4(c)]. When the adatom on the step site solidifies, it moves down to the front of the step site and solidifies there [Fig. 4(b)]. When an atom consisting the step melts and becomes an adatom, the adatom stays there with the probability 1/2 or moves onto the upper terrace with probability 1/2 if the destination is not occupied [Fig. 4(d)] (otherwise it cannot melt). Since the solidification occurs in both sides of the step, we set the melting probability twice as large as the previous permeable case. There is a small asymmetry in this algorithm: the probability of solidification from the upper terrace is approximately $(1 - c|_{\xi_+})$ times smaller than that onto the lower terrace and the probability of melting in the upper side terrace is approximately $(1 - c|_{\xi_-})$ times smaller than that onto the lower terrace. The

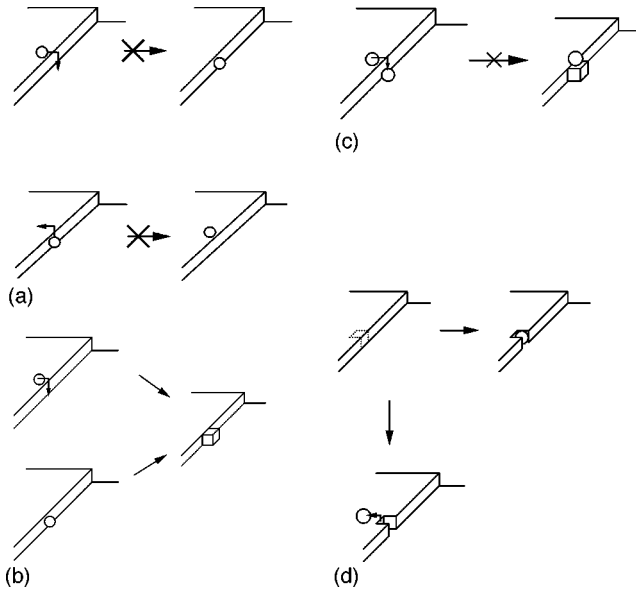


FIG. 4. Atomic processes at an impermeable step in the Monte Carlo simulation: (a) prohibition of the diffusion over the step, (b) solidification at the front site of the step, (c) prohibition of the solidification at the site occupied by another adatom, and (d) melting onto the upper and the lower terraces.

asymmetry decreases with decreasing adatom density. An estimate of the equilibrium density and the kinetic coefficients for the present algorithm are given in Appendix A.

Figure 5 shows time evolution of the step position in the Monte Carlo simulation. The parameters are $x_s = 16$, $c_{\text{eq}}^0 = 0.18$ ($\phi/k_B T = 1.5$), and $\tilde{\beta}/k_B T = 0.54$ ($\epsilon/k_B T = 1.0$). Since the step kinetics is fast $\lambda_- = 1.6 \times 10^{-2} \ll 1$ and $\lambda_+ = 1.9 \times 10^{-2}$, the amplification rate ω_q is approximately given by Eq. (4.6) and the critical drift velocity is $v_c^W \approx 8.4 \times 10^{-3}$. Figure 5(a) is the time evolution of the step position with the step-up drift ($v = -0.2$). As expected from the linear analysis, the step is more straight than that without the drift [Fig. 5(b)]. Figure 5(c) represents the time evolution with the step-down drift. Since the drift velocity $v = 0.2$ exceeds the critical value, the step is unstable and the wandering instability occurs. The wavelength of the fastest growing mode expected from Eq. (4.5) is estimated to $\lambda_{\text{max}} = 24$, which roughly agrees with the wavelength of the fluctuation observed in the initial stage of the instability. The unstable step produces peaks, which show chaotic motion similar to the permeable step.

B. Wandering instability in the vicinal face

When steps are straight and equidistant with a distance l , without the impingement of atoms, the adatom density on the terrace $0 \leq y \leq l$ is given by

$$c_0(y) = c_{\text{eq}}^0 e^{\tilde{v}l/2} \left(A \cosh \frac{\alpha y}{2x_s} + B \sinh \frac{\alpha y}{2x_s} \right), \quad (4.9)$$

where

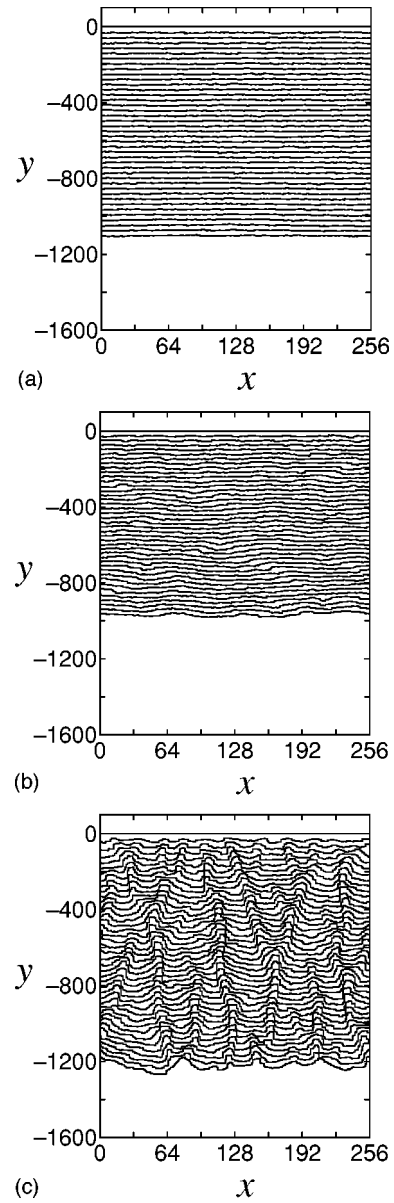


FIG. 5. Time evolution of the position of an impermeable step in sublimation (a) with the step-up drift ($v = -0.2$), (b) without the drift ($v = 0$), and (c) with the step-down drift ($v = -0.2$).

$$A = -\frac{1}{h_0(l)} \left[-\left(\frac{\lambda \tilde{v}}{2} \sinh \frac{\alpha \tilde{l}}{2} - \frac{\lambda \alpha}{2} \cosh \frac{\alpha \tilde{l}}{2} - \sinh \frac{\alpha \tilde{l}}{2} \right) + \frac{\lambda \alpha}{2} e^{-\tilde{v} \tilde{l}/2} \right], \quad (4.10)$$

$$B = -\frac{1}{h_0(l)} \left[\left(\frac{\lambda \tilde{v}}{2} \cosh \frac{\alpha \tilde{l}}{2} - \frac{\lambda \alpha}{2} \sinh \frac{\alpha \tilde{l}}{2} - \cosh \frac{\alpha \tilde{l}}{2} \right) + \left(1 + \frac{\lambda \tilde{v}}{2} \right) e^{-\tilde{v} \tilde{l}/2} \right], \quad (4.11)$$

$$h_0(l) = \lambda^2 \sinh \frac{\alpha \tilde{l}}{2} + \alpha \lambda \cosh \frac{\alpha \tilde{l}}{2} + \sinh \frac{\alpha \tilde{l}}{2}. \quad (4.12)$$

Since each terrace is treated separately, we can calculate the amplification rate ω_q with a general k . By using Eq. (4.9), the linear amplification rate is calculated as

$$\begin{aligned} \frac{\omega_q x_s^2}{\Omega D_s c_{eq}^0} = & \frac{u_+}{h_q(l)} \left[-\lambda^2(1+\tilde{q}^2) \sinh \frac{\alpha_q \tilde{l}}{2} - \frac{\lambda \alpha_q}{2} \cosh \frac{\alpha_q \tilde{l}}{2} - \frac{\lambda \tilde{v}}{2} \sinh \frac{\alpha_q \tilde{l}}{2} + \frac{\lambda \alpha_q}{2} e^{\tilde{v}\tilde{l}/2} \right] \\ & + \frac{u_-}{h_q(l)} \left[-\lambda^2(1+\tilde{q}^2) \sinh \frac{\alpha_q \tilde{l}}{2} - \frac{\lambda \alpha_q}{2} \cosh \frac{\alpha_q \tilde{l}}{2} + \frac{\lambda \tilde{v}}{2} \sinh \frac{\alpha_q \tilde{l}}{2} + \frac{\lambda \alpha_q}{2} e^{-\tilde{v}\tilde{l}/2} \right] + \frac{1}{h_q(l)} \left[\frac{\lambda \alpha_q u_+}{2} (e^{\tilde{v}\tilde{l}/2} e^{-i\tilde{k}\tilde{l}} - e^{\tilde{v}\tilde{l}/2}) \right. \\ & + \frac{\lambda \alpha_q u_-}{2} (e^{-\tilde{v}\tilde{l}/2} e^{i\tilde{k}\tilde{l}} - e^{-\tilde{v}\tilde{l}/2}) \left. \right] - \frac{1}{h_0(l)} \left(\lambda \alpha \cosh \frac{\alpha_q \tilde{l}}{2} - 2 \sinh \frac{\alpha_q \tilde{l}}{2} + \lambda \alpha \cosh \frac{\alpha_q \tilde{l}}{2} \right) \\ & - \frac{\Phi(l)}{h_q(l)} \left[2\lambda(1+\tilde{q}^2) \sinh \frac{\alpha_q \tilde{l}}{2} + \alpha_q \cosh \frac{\alpha_q \tilde{l}}{2} - \alpha_q \cosh \frac{\tilde{v}\tilde{l} - 2i\tilde{k}\tilde{l}}{2} \right] (1 - \cos \tilde{k}\tilde{l}) - \frac{\tilde{\Gamma}}{h_q(l)} \left[2\lambda(1+\tilde{q}^2) \sinh \frac{\alpha_q \tilde{l}}{2} \right. \\ & \left. + \alpha_q \cosh \frac{\alpha_q \tilde{l}}{2} - \alpha_q \cosh \frac{\tilde{v}\tilde{l} - 2i\tilde{k}\tilde{l}}{2} \right] \tilde{q}^2, \end{aligned} \quad (4.13)$$

where

$$\tilde{k} = kx_s \quad (4.14)$$

$$h_q(l) = \lambda^2(1+\tilde{q}^2) \sinh \frac{\alpha_q \tilde{l}}{2} + \alpha_q \lambda \cosh \frac{\alpha_q \tilde{l}}{2} + \sinh \frac{\alpha_q \tilde{l}}{2}, \quad (4.15)$$

$$u_+ = - \frac{x_s}{\lambda c_{eq}^0} \frac{dc_0}{dy} \Big|_{y=0} + \frac{1}{c_{eq}^0} c_0 \Big|_{y=0}, \quad (4.16)$$

$$u_- = - \frac{x_s}{\lambda c_{eq}^0} \frac{dc_0}{dy} \Big|_{y=l} - \frac{1}{c_{eq}^0} c_0 \Big|_{y=l}, \quad (4.17)$$

$$\Phi(l) = \frac{\Omega x_s}{k_B T} \frac{d^2 U}{dl^2} = \frac{\Omega x_s}{k_B T} \frac{6A}{l^4}. \quad (4.18)$$

Hereafter we consider the case that the step distance is much smaller than the surface diffusion length and that $\lambda \ll 1$. We expand Eq. (4.13) with l , and take account of the lowest order in l . For simplicity, we calculate ω_q for an in-phase fluctuation, $k=0$. When the step kinetics is slow enough to satisfy $\lambda \gg l/x_s$, the amplification rate for the long-wavelength fluctuation, ω_q , is given by²²

$$\frac{\omega_q x_s^2}{\Omega D_s c_{eq}^0} = \tilde{l}(\tilde{v} - \tilde{\Gamma}) \tilde{q}^2 + \dots \quad (4.19)$$

The equidistant train of steps is unstable with the step-down drift exceeding the critical value,

$$v_c^W = \frac{\Omega D_s \tilde{\beta}}{x_s^2 k_B T}, \quad (4.20)$$

which is one-fourth of v_c for an isolated step. With $\lambda \ll l/x_s$, the form of the amplification rate changes. In the

limit of fast step kinetics, $\lambda \rightarrow 0$, the step becomes permeable and we obtain the same result of as Eq. (3.21).

As shown in Table I, without the impingement of adatoms, the wandering instability occurs with the step-down drift for both the permeable and the impermeable steps. With the fast step kinetics, the difference due to the step permeability vanishes.

V. BUNCHING INSTABILITY OF THE PERMEABLE STEP

In the case of the permeable steps, the adatom densities of neighboring terraces are coupled by the boundary condition Eq. (3.1). In the step flow model, we must solve simultaneous equations to determine the adatom densities and it is difficult to study the bunching of many steps. Therefore we use a continuum model,⁴⁹ in which the drift of adatoms is readily taken into account. Recently Stoyanov¹² argued that a vicinal face consisting of permeable steps is unstable with the step-up drift, and showed that a large bunch is stabilized with the step-up drift. Here we analyze the linear stability of a vicinal face for a long-wavelength fluctuation, and give an analytical expression for the condition of the instability.

We neglect the fluctuation along steps and assume that the steps are straight. When the step distance is small compared with the characteristic length of modulation, we can describe the surface profile with the density of steps $\rho(y)$. Time evolution equations of the adatom density and the step density are given by^{12,49}

$$\frac{\partial c}{\partial t} = D_s \frac{\partial^2 c}{\partial y^2} - v \frac{\partial c}{\partial y} + F - \frac{1}{\tau} c - 2\rho K [c - c_{eq}(y)], \quad (5.1)$$

$$\frac{\partial \rho}{\partial t} + \frac{\partial}{\partial y} \{2\rho \Omega K [c - c_{eq}(y)]\} = 0, \quad (5.2)$$

where $c_{eq}(y)$ is the local equilibrium density of adatoms. Equation (5.1) is the diffusion equation including the effect of solidification of adatoms at the steps. The decrease of the

TABLE I. Conditions to induce instabilities.

Growth condition	Permeability	Terrace	Kinetics	Drift	Instability
sublimation	permeable	isolated	fast/slow	down	wandering
		$l/x_s \ll 1$	fast/slow	down	wandering
			not too slow ($\lambda \ll x_s/l$)	up	bunching
	impermeable	isolated	fast/slow	down	wandering
		$\alpha l/x_s \gg 1$	fast/slow	up	bunching
			$\alpha l/x_s \ll 1$	fast/slow	down
growth	permeable	isolated	fast/slow	up	wandering
		$l/x_{ms} \ll 1$	fast/slow	up	wandering
			not too slow ($\lambda \ll x_s/l$)	down	bunching
	impermeable	isolated	fast ($\lambda \ll 1$)	up	wandering
			slow ($\lambda \gg 1$)	down	wandering
		$\alpha l/x_s \gg 1$	fast ($\lambda \ll l/x_s$)	down	bunching
			slow ($\lambda \gg l/x_s$)	down	wandering /bunching
		$\alpha l/x_s \ll 1$	fast ($\lambda \ll l/x_s$)	up	wandering
				down	bunching
				slow ($\lambda \gg l/x_s$)	down

adatom density due to solidification is proportional to the local step density. Equation (5.2) is the continuity equation of the step density. The step current is ρV with the step velocity

$$V = 2\Omega K[c - c_{\text{eq}}(y)]. \quad (5.3)$$

Since we consider modulation only in the y direction, the curvature of the steps vanishes and the equilibrium adatom density is determined by the step interaction. The interaction force is derived from the step energy ξ as $f = -\partial\xi/\partial y$, and therefore^{50–52}

$$c_{\text{eq}} = c_{\text{eq}}^0 + \frac{\Omega c_{\text{eq}}^0}{k_B T} \frac{d\xi}{d\rho} \frac{\partial\rho}{\partial y} = c_{\text{eq}}^0 + \gamma(\rho) \frac{\partial\rho}{\partial y}. \quad (5.4)$$

The step energy $\xi(\rho)$ is given by Eq. (2.8) and

$$\frac{\partial\xi}{\partial\rho} = l^3 \frac{d^2 U}{dl^2} = 6A\rho, \quad (5.5)$$

which is the surface stiffness in y direction divided by a^2 . When the step density is uniform $\rho = \rho_0$, from Eqs. (5.1) and (5.2), the adatom density c_0 and the step velocity V_0 in the steady state are given by

$$c_0 = \frac{(F + 2\rho_0 K c_{\text{eq}}^0)\tau}{2\rho_0 K \tau + 1}, \quad (5.6)$$

$$V_0 = \frac{2\Omega K(F\tau - c_{\text{eq}}^0)}{2\rho_0 K \tau + 1}. \quad (5.7)$$

We study the linear stability of the vicinal face by giving a small perturbation to the step density, $\rho = \rho_0 + \delta\rho e^{iky + \omega_k t}$ and to the adatom density, $c(y) = c_0 + \delta c e^{iky + \omega_k t}$. Equations (5.1)–(5.4) determine the amplification rate ω_k via

$$\omega_k^2 + \left[k^2(D_s + 2\Omega\gamma\rho_0 K) + ik(V_0 + v) + \frac{1}{\tau} + 2\rho_0 K \right] \omega_k + \left(k^2 D_s + ikv + \frac{1}{\tau} \right) (2k^2 \Omega\gamma\rho_0 K + ikV_0) = 0. \quad (5.8)$$

There are two branches of solutions: $\omega_k = \omega(1) \rightarrow 0$ and $\omega_k = \omega(2) \rightarrow -1/\tau - \rho_0 K$ with $k \rightarrow 0$. Since the second mode decays much faster than the first one, the important amplification rate is the first one. The amplification rate is expressed as

$$\omega_k = i\nu_1 k + \nu_2 k^2 + i\nu_3 k^3 + \nu_4 k^4 + \dots \quad (5.9)$$

The real part of ω_k represents the amplification of the fluctuation. The instability for the long wavelength fluctuation is determined by ν_2 , which is given by

$$\nu_2 = \frac{V_0 \tau}{1 + 2\rho_0 K \tau} \left(v - \frac{V_0 + v}{1 + 2\rho_0 K \tau} \right) - \frac{2\Omega\rho_0 K \gamma(\rho_0)}{1 + 2\rho_0 K \tau}. \quad (5.10)$$

The second term is the effect of the step repulsion and always stabilizes the vicinal face. The first term in Eq. (5.10) can destabilize the vicinal face. If the step kinetics is very slow, $\rho_0 K \tau \rightarrow 0$, the first term is proportional to $-V_0^2 (< 0)$ and stabilizes the vicinal face. On the other hand, if the step kinetics is fast, $1 \ll \rho_0 K \tau$, i.e., $\lambda < x_s/l$, the first term can be positive. Then the coefficients in Eq. (5.9) are given by

$$\nu_1 = -\frac{V_0}{2\rho_0 \tau K},$$

$$\nu_2 = -\frac{2\Omega\rho_0 K \gamma(\rho_0) - v V_0 \tau}{2\rho_0 \tau K},$$

$$\nu_3 = -\frac{D_s V_0 \tau + 2\Omega\rho_0 K v \tau \gamma(\rho_0)}{2\rho_0 \tau K},$$

$$\nu_4 = -\frac{D_s \Omega \gamma(\rho_0)}{\rho_0}. \quad (5.11)$$

The amplification rate becomes positive when $V_0 v$ exceeds the critical value,

$$(V_0 v)_c = \frac{2\Omega \rho_0 K \gamma(\rho_0)}{\tau} = \frac{12\Omega^2 c_{\text{eq}}^0 K \rho_0^2}{k_B T \tau} A, \quad (5.12)$$

and the vicinal face is unstable. Since ν_4 is always negative, the vicinal face is still stable for the short-wavelength fluctuation. In sublimation, $V_0 < 0$, the instability occurs with the step-up drift. The drift direction to induce the bunching instability is opposite to that for the impermeable steps. Since the critical drift velocity is inversely proportional to the step velocity, with increasing the undersaturation, the bunching instability occurs more easily. The imaginary part of ω_k represents the propagation of the fluctuation. Near the threshold of the instability, the wave number of the fastest growing mode is small and the dominant term of the propagation in ω_k is $\nu_1 k$. The propagation velocity is $-\nu_1$, which is proportional to the step velocity V_0 and in the opposite direction to the step motion. Since $\rho K \tau \gg 1$, it is much slower than the motion of the steps.

Figure 6 represents snapshots of a step train in Monte Carlo simulation. The system size is 128×256 with 32 steps. Initially the steps are straight and equidistant. There is no impingement of adatoms, and the receding steps become unstable when the step-up drift exceeds the critical velocity v_c^B ,

$$v < v_c^B = -\frac{12\Omega K A}{k_B T l^3}. \quad (5.13)$$

The parameters in Fig. 6 are $l=8$, $x_s=16$, $c_{\text{eq}}^0=0.18$, $\tilde{\beta}/k_B T=0.54$ and $A/k_B T=4$. Then the critical drift velocity v_c^B is calculated as $v_c^B = -0.19$. Figures 6(a) and 6(b) show snapshots with the step-up drift. The drift velocity is $v = -0.6$, and step bunching occurs. In the initial stage of the bunching [Fig. 6(a)], the long-wavelength fluctuation of the step distance appears. In the late stage [Fig. 6(b)], the bunches collide with each other and large bunches appear. When we carry out the simulation in a larger system (the system size is 512×512 , with 64 steps), the bunches wander and sometimes collide with neighboring bunches [Fig. 6(c)]. The pattern is similar to the form of bunches observed in the experiment³ and the one in the simulation of a simplified step model.¹⁷ Figures 6(d) and 6(e) show snapshots of the step bunching without the repulsive interaction, where only the formation of multiheight steps is forbidden. In the initial stage [Fig. 6(d)], the step train is unstable for a short-wavelength fluctuation, and bunches consisting of a few steps wander. In spite of such a large difference in the initial stage, large bunches appear in the late stage [Fig. 6(e)]. Because of a lack of repulsive interaction, the step distance in the bunches is smaller than that with repulsion.

VI. BUNCHING INSTABILITY OF THE IMPERMEABLE STEP

To study the bunching of impermeable steps, we use the same model as that used in Sec. IV. The diffusion equation is

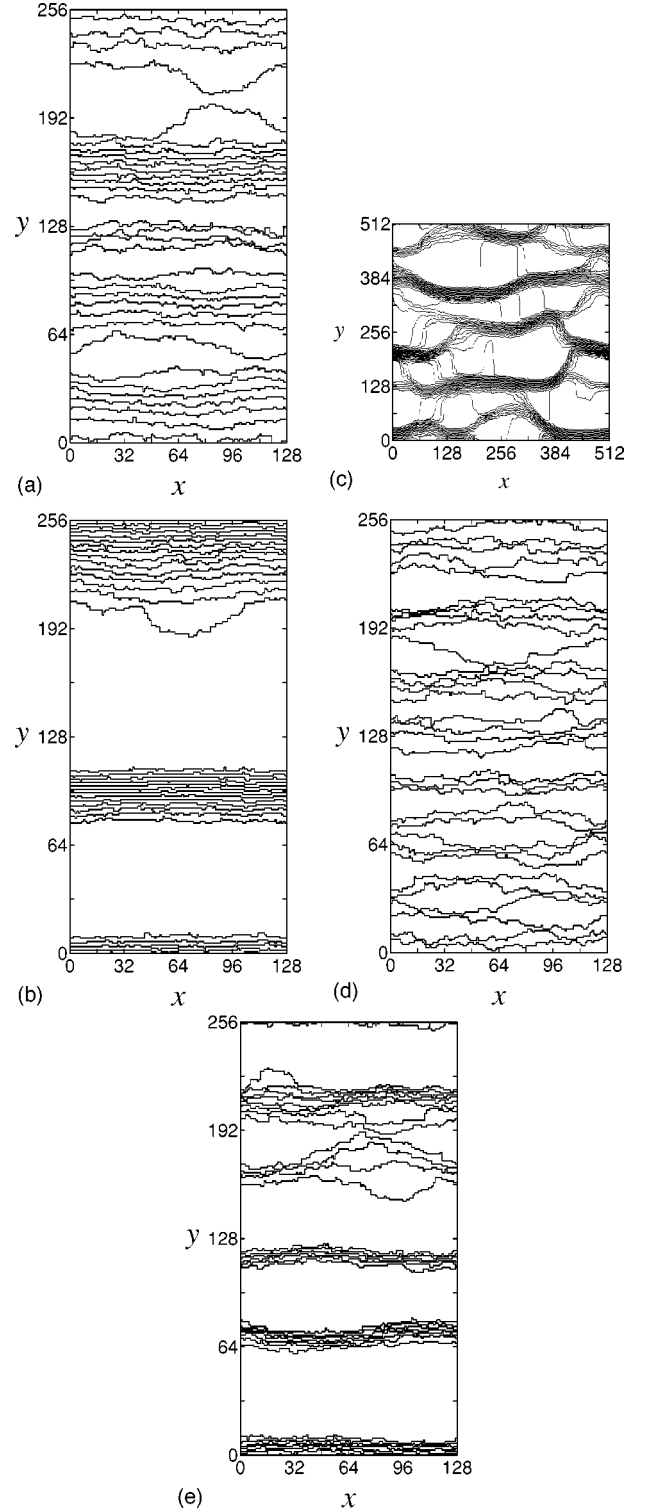


FIG. 6. Snapshots of bunching of permeable steps in sublimation: (a) in the initial stage ($t = 5.6 \times 10^4$), (b) in the late stage ($t = 8.2 \times 10^4$), and (c) in the late stage ($t = 1.0 \times 10^5$) in a large system, with the step-up drift ($v = -0.6$) and repulsive interaction ($A/k_B T = 4.0$). (d) In the initial stage ($t = 4.1 \times 10^3$), and (e) in the late stage ($t = 2.1 \times 10^4$), with the step-up drift ($v = -0.6$) and no repulsive interaction.

given by Eq. (2.2), and the boundary conditions are Eqs. (4.1) and (4.2). The linear stability is studied in Ref. 16, and here we summarize the result. When the impingement of the adatoms is negligible, the velocity of the m th step V_0^m is

given by

$$\frac{2x_s V_0^m}{\Omega D_s} = \frac{[(-2\lambda - \tilde{v}) \sinh(\alpha \tilde{l}_+/2) - \alpha \cosh(\alpha \tilde{l}_+/2)] c_n + \alpha e^{-\tilde{v} \tilde{l}_+/2} c_{n+1}}{(1 + \lambda^2) \sinh(\alpha \tilde{l}_+/2) + \alpha \lambda \cosh(\alpha \tilde{l}_+/2)} + \frac{[(-2\lambda + \tilde{v}) \sinh(\alpha \tilde{l}_-/2) - \alpha \cosh(\alpha \tilde{l}_-/2)] c_n + \alpha e^{\tilde{v} \tilde{l}_-/2} c_{n-1}}{(1 + \lambda^2) \sinh(\alpha \tilde{l}_-/2) + \alpha \lambda \cosh(\alpha \tilde{l}_-/2)}, \quad (6.1)$$

where \tilde{l}_\pm are the scaled width of the upper side (-) and the lower side (+) terraces, and $\tilde{l}_\pm = |\zeta_{m\pm 1} - \zeta_m|/x_s$. The equilibrium adatom density at the m th step c_m is given by Eq. (5.4). For the small perturbation $\delta y_m = \delta y_k e^{im\tilde{k}\tilde{l} + \omega_k t}$ to the straight steps, the amplification rate ω_k is given by

$$\frac{\tau \operatorname{Re} \omega_k}{\Omega c_{\text{eq}}^0} = [\mu_1(l) - \mu_2(l) \Phi(l)] \sin^2 \frac{\tilde{k}\tilde{l}}{2}, \quad (6.2)$$

$$\frac{\tau \operatorname{Im} \omega_k}{\Omega c_{\text{eq}}^0} = [\sigma_1(l) - \sigma_2(l) \Phi(l)] \sin \tilde{k}\tilde{l}, \quad (6.3)$$

where the coefficients are¹⁶

$$\mu_1(l) = 2 \frac{d}{d\tilde{l}} \left[\frac{\tilde{v} \sinh(\alpha \tilde{l}/2) + \alpha \cosh(\alpha \tilde{l}/2)}{(1 + \lambda^2) \sinh(\alpha \tilde{l}/2) + \alpha \lambda \sinh(\alpha \tilde{l}/2)} \right], \quad (6.4)$$

$\mu_2(l)$

$$= 4 \frac{2\lambda \sinh(\alpha \tilde{l}/2) + \alpha \cosh(\alpha \tilde{l}/2) - \alpha \cosh(\tilde{v} \tilde{l}/2) \cos \tilde{k}\tilde{l}}{(1 + \lambda^2) \sinh(\alpha \tilde{l}/2) + \alpha \lambda \cosh(\alpha \tilde{l}/2)}, \quad (6.5)$$

$$\sigma_1(l) = \frac{d}{d\tilde{l}} \left[\frac{2\lambda \sinh(\alpha \tilde{l}/2) + \alpha \cosh(\alpha \tilde{l}/2) - \alpha \cosh(\tilde{v} \tilde{l}/2)}{(1 + \lambda^2) \sinh(\alpha \tilde{l}/2) + \alpha \lambda \cosh(\alpha \tilde{l}/2)} \right], \quad (6.6)$$

$$\sigma_2(l) = \frac{2\alpha \sinh(\tilde{v} \tilde{l}/2) (1 - \cos kl)}{(1 + \lambda^2) \sinh(\alpha \tilde{l}/2) + \alpha \lambda \cosh(\alpha \tilde{l}/2)}. \quad (6.7)$$

When the step distance is small, $\alpha l/2x_s \ll 1$, Eq. (6.4) is approximated by

$$\mu_1(l) = \frac{2\tilde{v}\lambda}{[(1 + \lambda^2)\tilde{l}/2 + \lambda]^2}, \quad (6.8)$$

which is proportional to \tilde{v} . The bunching instability is induced by the step-down drift if it wins the repulsive interaction. A simple formula is obtained if $l/x_s \ll \lambda \sim 1$: Eq. (6.2) becomes¹⁶

$$\frac{\tau \operatorname{Re} \omega_k}{\Omega c_{\text{eq}}^0} = \left[\frac{2\tilde{v}}{\lambda} - 4\Phi(l) \left(\tilde{l} + \frac{1 - \cos \phi}{\lambda} \right) \right] \sin^2 \frac{\tilde{k}\tilde{l}}{2} \approx \left(\frac{\tilde{v}}{2\lambda} - \Phi(l)\tilde{l} \right) \tilde{l}^2 \tilde{k}^2 - \frac{\Phi(l)}{2\lambda} \tilde{l}^4 \tilde{k}^4 + \dots \quad (6.9)$$

The coefficient of k^4 is determined by the repulsive interaction potential, and is negative. The vicinal face is stable for the short-wavelength fluctuation. When the drift is in the step-down direction and its velocity exceeds the critical value,

$$v_c^B = \frac{12\lambda D_s \Omega A}{x_s l^3 k_B T}, \quad (6.10)$$

the coefficient of k^2 is positive, and the vicinal face becomes unstable for the long-wavelength fluctuation.

In the above analysis we supposed that the steps are straight. If the step distance is small, however, the step wandering is also induced by the step-down drift. Figure 7 shows snapshots of a step train with a small step distance in Monte Carlo simulation. The system size is 128×256 and the number of steps is 32. Initially the steps are equidistant and $l = 8$. The parameters are $x_s = 16$, $\tilde{\beta} = 1.35$, $c_{\text{eq}}^0 = 0.18$, and $A/k_B T = 4$. Figure 7(a) shows a snapshot of the step train with step-up drift ($v = -0.3$) at $t = 1.8 \times 10^4$. As expected from the linear analysis, neither the wandering nor the bunching occurs. When the drift is in the step-down direction ($v = 0.3$), both the bunching and the wandering occur simultaneously [Figs. 7(b) and 7(c)]. In the initial stage [Fig. 7(b)], step wandering accompanied by bunching with short length occurs. The short bunches grow and the bunches are connected to each other [Fig. 7(c)], which is very different from bunching of permeable steps (Fig. 6). Though the wandering and bunching are induced simultaneously in Fig. 7, when we use appropriate parameters, the bunching [Fig. 8(a), with a large stiffness] or the wandering [Fig. 8(b), with a small stiffness and a strong repulsion] is induced separately.

Figure 9 contains a snapshot of a step train with the distance longer than the surface diffusion length, $l/x_s = 2$. The equidistant step train with a large step distance is unstable with the step-up drift. The linear instability with a large step distance is studied by the one-dimensional step flow model.^{9,10,16} With increasing step distance, the drift direction to induce the step bunching changes and the equidistant step train is unstable with the step-up drift. Since the step train with a small step distance is stable with the step-up drift, tight bunches are not produced. Thus the result of simulation

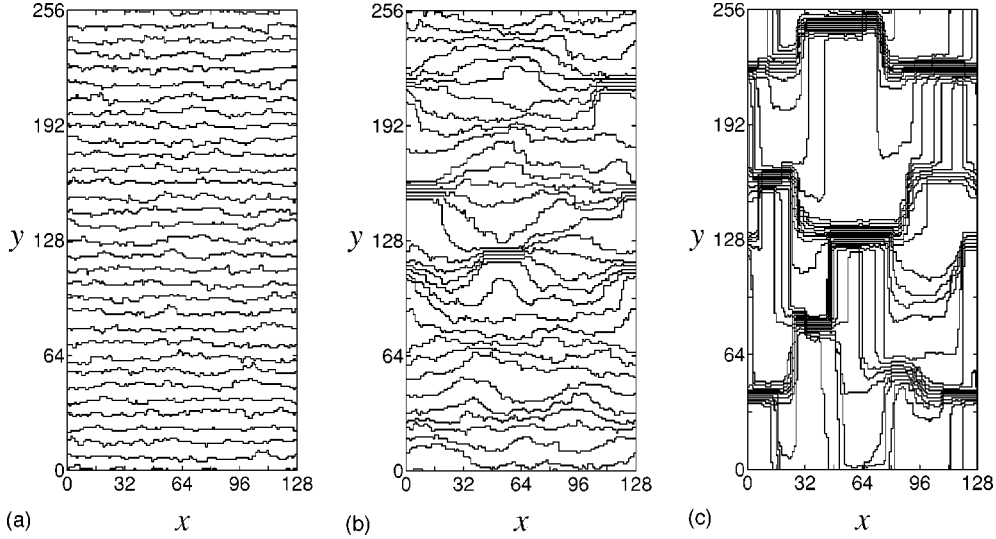


FIG. 7. Snapshots of impermeable steps with the repulsive interaction ($A/k_B T = 4$) in sublimation: (a) stable ($t = 1.8 \times 10^4$), with the step-up drift ($v = -0.4$); (b) in the initial stage of bunching ($t = 1.0 \times 10^4$); and (c) in the late stage ($t = 1.8 \times 10^4$), with the step-down drift ($v = 0.4$).

is in agreement with the previous study.^{9,10,16} Since the steps are stable for wandering, they are straight in Fig. 9.

VII. INSTABILITIES IN GROWTH

Recently, step bunching during growth with the direct electric current is observed by Yang *et al.*⁵ in the low-temperature range ($T \sim 945^\circ\text{C}$) and by Métois and Stoyanov¹³ both in the middle-temperature range ($1160^\circ\text{C} \leq T \leq 1240^\circ\text{C}$) and in the high-temperature range ($1260^\circ\text{C} \leq T \leq 1320^\circ\text{C}$). In the latter experiment the reversal of the current direction, which is observed in sublimation, did not occur. In this section we summarize our result of investigation for the instabilities in growth. We calculate the linear amplification rate for the long-wavelength fluctuation. We also show the result of Monte Carlo simulation, which was performed in several cases to test the linear stability analysis. The full expressions of the amplification rate are presented in the Appendixes.

A. Wandering instability of permeable steps

If the step is perfectly permeable, the amplification rate for an isolated step is given by Eq. (B5),

$$\frac{\omega_q x_s^2}{\Omega c_{\text{eq}}^0 D_s} = \frac{1}{2(1+\lambda)} \left[\frac{-\Delta\tilde{F}\tilde{v}}{(1+\lambda)} - 4\tilde{\Gamma} \right] \tilde{q}^2 + \dots, \quad (7.1)$$

where $\Delta\tilde{F} = (F\tau/c_{\text{eq}}^0 - 1)$ and terms of order \tilde{v}^2 has been neglected. Since $\Delta\tilde{F} > 0$ in growth, the wandering instability is induced by the step-up drift in contrast to the sublimation case. Figure 10 shows the time evolution of an isolated permeable step obtained by Monte Carlo simulation. The parameters are $\tilde{\beta}/k_B T = 1.35$, $c_{\text{eq}}^0 = 0.18$, $x_s = 16$, and $F = 2 \times 10^{-3}$. The critical drift velocity expected from Eq. (7.1) is $v_c^W = -0.12$. When the drift is in the step-down direction ($v = 0.2$), the step is stable [Fig. 10(a)] and straighter than that without drift [Fig. 10(b)]. When the velocity of the step-up drift is $v = -0.2$, wandering instability occurs [Fig.

10(c)]. From Eq. (B1) the wavelength of the most unstable mode is calculated as $\lambda_{\text{max}} = 33$, which roughly agrees with the typical wavelength of the step wandering in the early stage of the simulation. The wavelength of the wandering in the late stage is larger than that. The unstable step produces grooves, and their motion is chaotic in space and time. The pattern is similar to the solution of the KS equation (3.14) with a positive coefficient δ of the nonlinear term.²⁴

For the wandering in a vicinal face, the amplification rate is given by Eq. (B9):

$$\frac{\omega_q}{\Omega D_s c_{\text{eq}}^0} = \left(\frac{-\Delta\tilde{F}\tilde{v}\tilde{l}^5}{360} - \tilde{\Gamma}\tilde{l} \right) q^2 + \dots \quad (7.2)$$

The difference between ω_q in sublimation [Eq. (3.21)] and that in growth [Eq. (7.2)] is the prefactor $-\Delta\tilde{F}$ in front of the drift term. In growth, the wandering instability occurs with the step-up drift irrespective of the step kinetics λ .

B. Wandering instability of impermeable steps

If the step is impermeable, the amplification rate for an isolated step is given by Eq. (C1). If the step kinetics is fast $\lambda \ll 1$ and \tilde{v}^2 is negligible, the amplification rate in growth is obtained by replacing \tilde{v} in the amplification rate in sublimation [Eqs. (3.9) and (3.11) with $\lambda = 0$] with $-\Delta F\tilde{v}$:

$$\frac{\omega_q x_s^2}{\Omega c_{\text{eq}}^0 D_s} = -\frac{\Delta\tilde{F}\tilde{v} + 4\tilde{\Gamma}}{2} \tilde{q}^2 - \frac{-\Delta\tilde{F}\tilde{v} + 8\tilde{\Gamma}}{8} \tilde{q}^4. \quad (7.3)$$

In growth the instability can occur with the step-up drift ($\tilde{v} < 0$). Figure 11 shows the time evolution of an isolated impermeable step in the fast kinetics. The system size is 256×256 and the parameters are $x_s = 16$, $\tilde{\beta}/k_B T = 1.35$, $c_{\text{eq}}^0 = 0.18$, and $F = 2 \times 10^{-3}$. From Eq. (7.3) the critical drift velocity is given by $v_c^W = -1.1 \times 10^{-2}$. Figure 11(a) represents the time evolution of a stable step with the step-down drift ($v = 0.2$). As expected from the linear analysis, the step

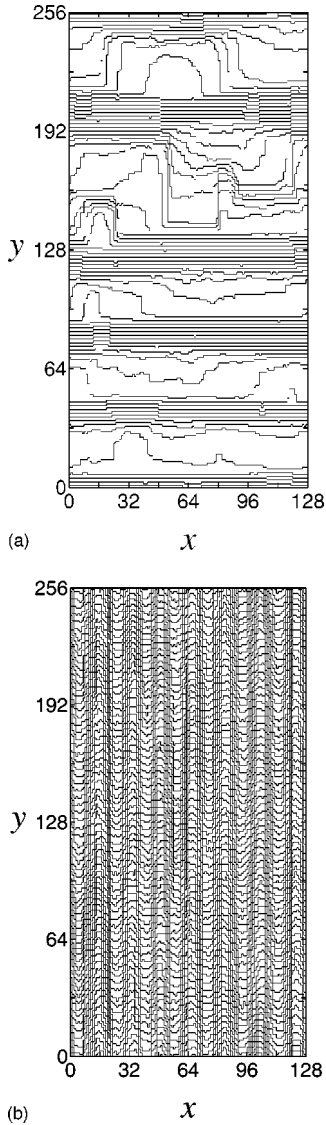


FIG. 8. Snapshots of impermeable steps in sublimation: (a) Bunching of straight steps with $A/k_B T = 8$, $l = 4$, $x_s = 8$, $c_{\text{eq}} = 0.18$, $\tilde{\beta}/k_B T = 2.76$, and $v = 0.4$ at $t = 9.5 \times 10^3$. (b) Wandering of an equidistant step train with $A/k_B T = 64$, $l = 4$, $x_s = 8$, $c_{\text{eq}} = 0.18$, $\tilde{\beta}/k_B T = 0.13$, and $v = 0.4$ at $t = 1.8 \times 10^4$.

is straighter than that without drift [Fig. 11(b)]. Figure 11(c) represents the time evolution of an unstable step with the step-up drift ($v = -0.2$). The unstable step produces the chaotic pattern similar to the permeable step.

If the step kinetics is slow $\lambda \gg 1$, the first term in Eq. (C1) may be neglected, and the amplification rate is given by

$$\frac{\omega_q x_s^2}{\Omega c_{\text{eq}}^0 D_s} \approx \frac{1}{\lambda} (\tilde{F}\tilde{v} - 2\tilde{\Gamma}) \tilde{q}^2 + \dots, \quad (7.4)$$

where $\tilde{F} = F\tau/c_{\text{eq}}^0$. The destabilizing effect is proportional to $\tilde{F}\tilde{v}$, which comes from the second term in Eq. (C1). Whether the surface is in sublimation or in growth, the wandering instability occurs with step-down drift in the slow step kinetics. The critical drift velocity is independent of the step kinetic coefficient in growth (if λ is large enough), while it is proportional to λ in sublimation ($F = 0$).

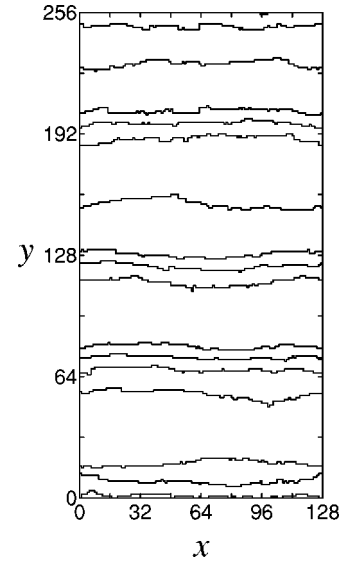


FIG. 9. A snapshot of the weak bunching of the impermeable step in sublimation at $t = 3.7 \times 10^4$. The step distance is longer than the surface diffusion length, $l = 16$ and $x_s = 8$. The other parameters are $A/k_B T = 10$, $c_{\text{eq}} = 0.18$, and $\tilde{\beta}/k_B T = 2.76$.

For the wandering in a vicinal face, with $l/x_s \ll \lambda$, the amplification rate is given by Eq. (C12),

$$\frac{\omega_q x_s^2}{\Omega D_s c_{\text{eq}}^0} = \tilde{l}(\tilde{v} - \tilde{\Gamma}) \tilde{q}^2 + \dots, \quad (7.5)$$

which is the same as that in sublimation equation (4.19). The step distance is so short that the impingement F does not influence the instability. In the limit of fast step kinetics, on the other hand, the amplification rate is again given by Eq. (C13), which does not differ from the permeable case [Eq. (3.21)]. Because of the short circuit [Fig. 1(d)], the steps are effectively permeable. The instability occurs with the step-up drift in growth.

For impermeable steps, the drift direction to induce the wandering instability changes with the step kinetics. If the step kinetics is fast, $\lambda \ll 1$ or $\lambda \ll l/x_s$, the drift direction to induce the instability in growth is opposite to that in sublimation. If the step kinetics is slow, $\lambda \gg 1$ or $\lambda \gg l/x_s$, the drift direction to induce the instability does not change.

C. Bunching instability of permeable steps

The amplification rate of fluctuation in the step density for permeable steps has been already given by Eq. (5.9). In growth ($V_0 > 0$), the bunching is induced by the step-down drift. Figure 12 shows some results of the Monte Carlo simulation for permeable steps in growth. The system size is 128×256 , and the number of steps is 32. The parameters are $\tilde{\beta}/k_B T = 1.35$, $c_{\text{eq}}^0 = 0.18$, $F = 2 \times 10^{-3}$, and $A/k_B T = 10$. The critical drift velocity is estimated as $v_c^B = 0.13$. Figures 12(a) and 12(b) represent the step bunching with the step-down drift ($v = 0.4$). In the initial stage ($t = 9.6 \times 10^4$) [Fig. 12(a)], the equidistant step train becomes unstable for the long-wavelength fluctuation. Later at $t = 1.9 \times 10^5$ [Fig. 12(b)], the contrast of the step density becomes clear, and large bunches appear. Since the wandering occurs with the

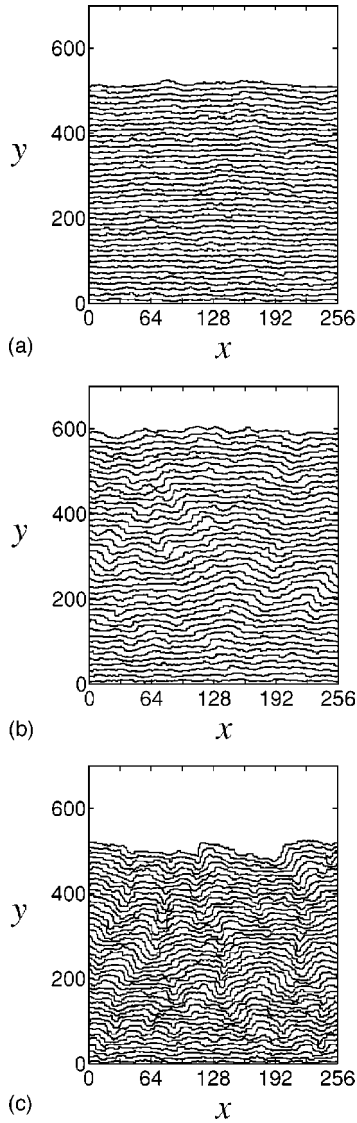


FIG. 10. Time evolution of the position of a permeable step in growth. The impingement rate is $F = 2 \times 10^{-3}$, (a) with the step-up drift ($v = -0.2$), (b) without the drift, and (c) with the step-down drift ($v = 0.2$).

drift of the opposite direction, the steps in the bunches are rather straight. Figure 12(c) represents the stable step train with $v = -0.4$. Though the drift is in the step-up direction, the wandering instability does not occur because of the large critical drift velocity $v_c^W = 16.9$ estimated from Eq. (7.2).

D. Bunching instability of impermeable steps

If steps are impermeable, the difference of the amplification rate in sublimation and in growth appears in $\mu_1(l)$ and $\sigma_1(l)$ of Eqs. (6.2) and (6.3). When the step distance is small, $al/2x_s \ll 1$, $\mu_1(l)$ is given by Eq. (D4)

$$\mu_1(l) \approx \frac{2\tilde{v}\lambda}{[(\lambda^2 + 1)\tilde{l}/2 + \lambda]^2}, \quad (7.6)$$

which does not depend on the impingement rate F . The step distance is so short that the effect of impingement is negligible. Thus the drift direction to induce the bunching does

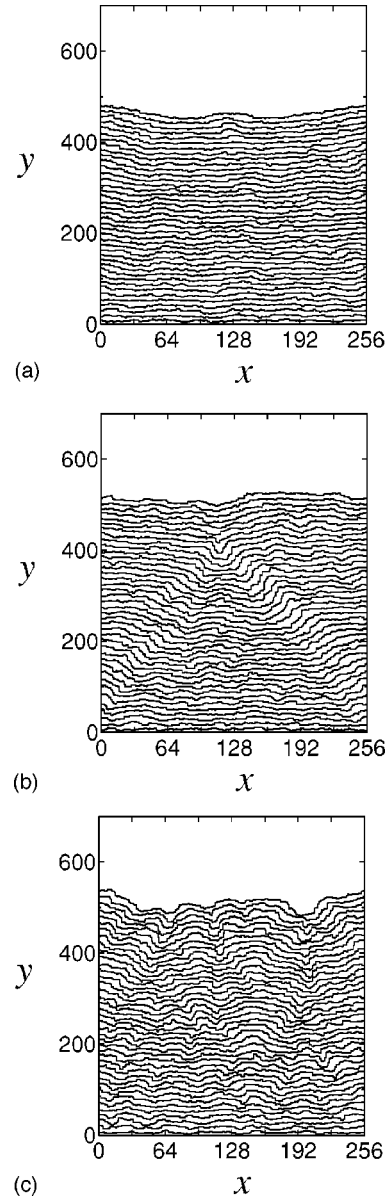


FIG. 11. Time evolution of the position of an impermeable step in growth. The impingement rate is $F = 2 \times 10^{-3}$, (a) with the step-down drift ($v = 0.2$), (b) without drift, and (c) with the step-up drift ($v = -0.2$).

not change in growth and in sublimation. When the step distance is long $al/2x_s \gg 1$, Eq. (D2) is positive with the step-down drift in growth.¹⁶ Thus the equidistant step train is unstable with the step-down drift in growth. The drift direction to induce the bunching changes in growth and in sublimation with a long step distance.

Figure 13 shows the bunching of impermeable steps with fast kinetics $K_+ = 3.3$ and $K_- = 3.9$ in growth. The system size is 128×256 , and the number of the steps is 32. The parameters are $\tilde{\beta}/k_B T = 1.35$, $c_{\text{eq}}^0 = 0.18$, $F = 2 \times 10^{-3}$, and $A/k_B T = 15$. The vicinal face is unstable with the step-down drift [Figs. 13(a) and 13(b)]. Long bunches appear in the late stage [Fig. 13(b)] in contrast to Fig. 7(c), where both bunching and wandering occur. The fluctuation of the bunches is larger than that of the permeable steps [Fig. 12(b)]. When the drift is in the step-up direction, the vicinal face is stable and

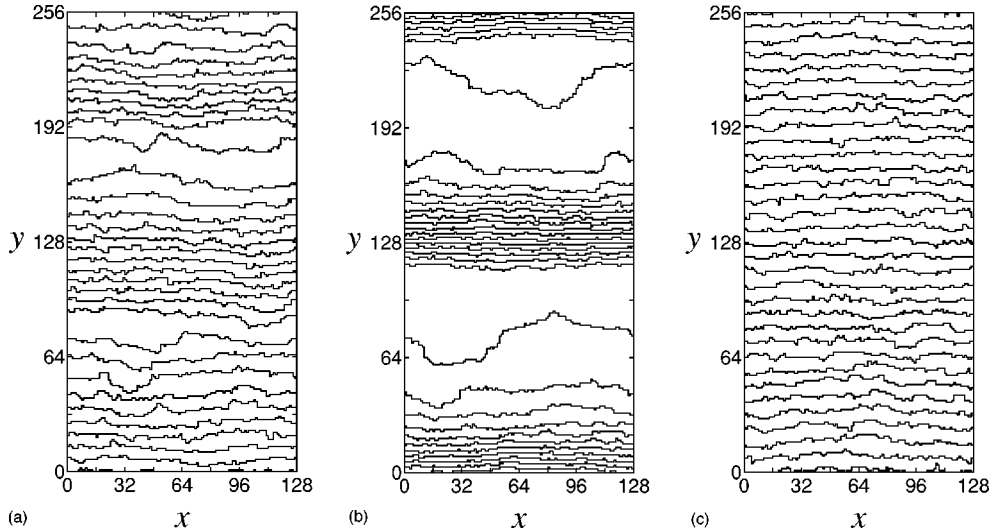


FIG. 12. Snapshots of bunching of permeable steps with the repulsive interaction $A/k_B T = 10$ in growth, (a) in the initial stage ($t = 9.6 \times 10^4$) and (b) in the late stage ($t = 1.9 \times 10^5$) with the step-down drift ($v = 0.4$), and (c) at $t = 3.8 \times 10^4$ with the step-up drift ($v = -0.4$),

the train of straight step is equidistant [Fig. 13(c)]. Figure 14 contains a snapshot of the bunching of impermeable steps with the long step distance, $\alpha/lx_s \gg 1$. The system size is 128×256 and the number of steps is 16. The parameters are $K_+ = 3.3$, $K_- = 3.9$, $x_s = 16$, $\tilde{\beta}/k_B T = 2.76$, $c_{\text{eq}}^0 = 0.18$, $F = 5 \times 10^{-3}$, and $A/k_B T = 10$. Steps are also unstable with the step-down drift. The drift direction to induce the bunching remains the same as that with a small step distance. The fluctuation of steps is large because of the large step distance.

In growth, the step bunching occurs with the step-down drift for both permeable and impermeable steps. The reversal of the drift direction to induce the bunching does not occur with growth.

VIII. DISCUSSION

The conditions to induce instabilities are summarized in Table I. The physical reasons for these instabilities in a vicinal face ($l \ll x_s$) are the following. The bunching of permeable step is explained by the change of adatom density.¹² With the step-up drift in sublimation, if the step density is high in some region the adatom density increases there due to the melting, and the high-adatom-density region is conveyed to the upper part of the vicinal face and decelerates the steps there. Steps are accumulated, and the density fluctuation is amplified. With the step-down drift in growth, conversely, the adatom density in the high-step-density region becomes low, and the steps in the lower part are decelerated.¹³ Thus steps are also accumulated. The bunching of impermeable steps is explained by the change of the terrace width.⁴⁴ Due to the drift, neglecting the asymmetry in the step kinetics, a step that has a larger terrace in the downstream moves faster in sublimation. In growth, conversely, a step that has a larger terrace upstream moves faster. In both cases a step overtakes the next one if the drift is in the step-down direction, and a step pairing occurs. Repulsive interaction between steps changes the pairing instability to the instability of the step density.⁴⁷ The bunching instability is a

result of the change of the step velocity, which is determined by the total current flowing into (or out from) the step. The wandering instability is a Mullins-Sekerka instability, which is controlled by the diffusion current at the step. Irrespective of the step permeability the gradient of the adatom density is steeper in the up-stream direction. Thus the diffusion current in this direction is dominant, and the wandering instability occurs if the up-stream direction coincides with the step motion:⁴² with the step-down drift in sublimation and with the step-up drift in growth (if the step kinetics is too slow, $\lambda \gg 1$, this simple argument does not hold).

In experiment the current direction to induce the bunching reverses several times in sublimation:^{2-5,26} the bunching occurs with the step-down current in the low- and high-temperature ranges, and with the step-up current in the middle-temperature range. In growth,^{5,13} however, the reversal does not occur, and the bunching is always induced by the step-down current. The wandering is observed in the middle temperature range with the step-down drift,²⁶ which is opposite to the current direction to induce the step bunching. All these results are explained if the steps, with $\alpha/lx_s \ll 1$, are impermeable in the low- and high-temperature ranges, and permeable in the middle-temperature range, with a positive effective charge irrespective of temperature as proposed by Stoyanov.¹² Very recently, Degawa *et al.*²³ found, by observation of the change of a surface profile, that the drift is always in the direction of the electric current. This report also supports the present explanation.

In a Si(111) vicinal face, the surface diffusion length is $x_s = 1.3 \times 10^6$ Å, and the diffusion constant is $D_s = 1.8 \times 10^{10}$ Å²/s at 945 °C (in the low-temperature range), and $x_s = 5.7 \times 10^4$ Å and $D_s = 1.6 \times 10^{11}$ Å²/s at 1273 °C (in the high-temperature range).⁵ The scaled drift velocity \tilde{v} is given by $\tilde{v} = x_s Z_{\text{eff}} e E / k_B T$, where $Z_{\text{eff}} e$ is the effective charge and E is the electric field. When $E = 500$ V/m, which is a typical value, and $Z_{\text{eff}} = 0.1$, the scaled drift velocity \tilde{v} is estimated to be $\tilde{v} = 0.06$ at 945 °C and $\tilde{v} = 0.002$ at 1273 °C. Since the typical step distance in the experiments^{2-5,13,26} is $l \leq 4000$

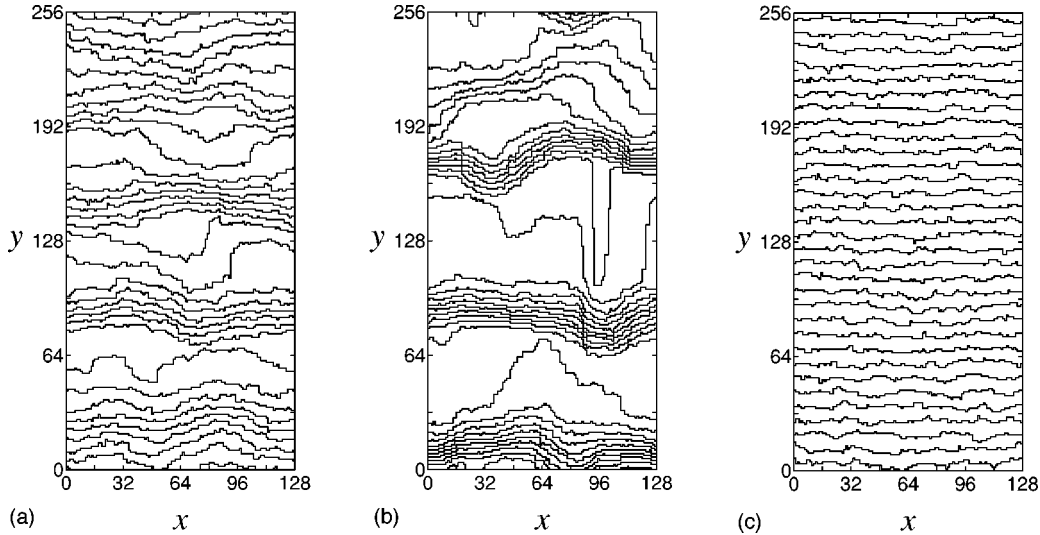


FIG. 13. Snapshots of impermeable steps in growth. The initial step distance is $l=8$, with $x_s=16$. Bunching (a) in the initial stage ($t=1.9\times 10^4$) and (b) in the late stage ($t=3.1\times 10^4$) with the step-down drift ($v=0.2$), and (c) a stable train with the step-up drift ($v=-0.2$) at $t=3.1\times 10^4$.

\AA , $\alpha l/x_s \ll 1$ is satisfied. At 1190°C , where bunching occurs with the step-up current in sublimation, the parameters are estimated as $D_s=1.0\times 10^{11}\text{ \AA/s}$ and $x_s=1.0\times 10^5\text{ \AA}$. If bunching occurs with a step distance $l \geq 10^3\text{ \AA}$, the kinetic coefficient is $K > 5\times 10^3\text{ \AA/s}$ with a perfectly permeable step. Since the estimation of K by using the impermeable model is $K \approx 5.5\times 10^7\text{ \AA/s}$,⁵ bunching occurs with a much smaller kinetic coefficient if the steps are perfectly permeable.

In the Monte Carlo simulation, we only take account of step interaction in the y direction. When bunches are straight as in the permeable case, this simulation is valid, and bunches similar to that in the experiments are obtained. When the bunches bend and become parallel to the y axis as

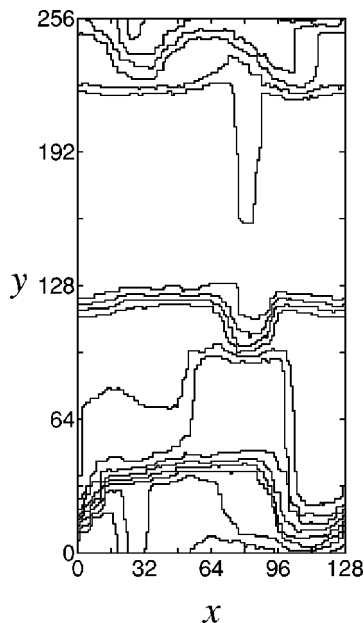


FIG. 14. Snapshots of bunching of impermeable steps in growth with the step distance longer than the surface diffusion length. The drift is in the step-down direction ($v=0.2$), and $t=8.8\times 10^3$.

in the impermeable case we found in the sublimation, we need to take account of the step interaction in all directions and to remove the SOS condition. For the particular case where both bunching and wandering occur simultaneously, we have derived a two-dimensional continuum model to describe the surface morphology.²² By numerical integration of the continuum evolution equation we have found domains of diagonal ridges. The correlated pattern of bunching and wandering in Fig. 7(c) is reminiscent of this ridge pattern. However, to obtain realistic surface pattern in a Monte Carlo simulation, we need to use a more realistic model and to perform larger scale simulation.

ACKNOWLEDGMENTS

This work was performed as a part of the program ‘‘Research for the Future’’ of the Japanese Society for the Promotion of Science, and supported by a Grant in Aid from the Ministry of Education of Japan. The authors benefited from the interuniversity cooperative research program of Institute for Materials Research, Tohoku University.

APPENDIX A: KINETIC COEFFICIENT IN THE MONTE CARLO SIMULATION

In the lattice model simulation for the impermeable step, the average number of atoms that solidify in a unit time increment (one diffusion step) Δt from the lower terrace is

$$\Delta N_s^+ = \frac{Lc_+}{N_a} p_s, \quad (\text{A1})$$

and that from the upper terrace is

$$\Delta N_s^- = \frac{Lc_-}{N_a} (1 - c_+) p_s, \quad (\text{A2})$$

where L is the system size (the step length in the x direction), N_a is the number of adatoms, and p_s is the average solidification probability:

$$p_s = \frac{1}{1 + e^{-\phi/k_B T}}. \quad (\text{A3})$$

The average number of melting atoms that go onto the lower terrace is

$$\Delta N_m^+ = \frac{L}{N_a} (1 - c_-) p_m \frac{1}{2}, \quad (\text{A4})$$

and the number that go onto the upper terrace is

$$\Delta N_m^- = \frac{L}{N_a} (1 - c_-) p_m \frac{1}{2} (1 - c_-), \quad (\text{A5})$$

where p_m is the average melting probability:

$$p_m = \frac{2}{1 + e^{\phi/k_B T}}. \quad (\text{A6})$$

To balance the solidification from both sides of the step, the melting of adatoms should occur twice as frequently as that of the permeable step, and p_m should be twice as large as that of the permeable step. In the equilibrium state $c_+ = c_-$, and the conditions $\Delta N_s^+ = \Delta N_m^+$ and $\Delta N_s^- = \Delta N_m^-$ give the equilibrium density

$$c_{\text{eq}+} = c_{\text{eq}-} = c_{\text{eq}} = \frac{1}{1 + e^{\phi/k_B T}}, \quad (\text{A7})$$

which is equal to the equilibrium adatom density in the permeable case. If c_+ and c_- deviate from this value, the net number of solidifying atoms from the lower terrace per unit length, in the linear approximation, is

$$\frac{\Delta N_s^+ - \Delta N_m^+}{L} = \frac{p_s}{N_a} (c_+ - c_{\text{eq}}) + \frac{p_m}{2N_a} (c_- - c_{\text{eq}}), \quad (\text{A8})$$

where we have used the equilibrium condition [Eq. (A7)]. This number depends not only on c_+ but also on c_- , which differs from boundary condition (4.1). It is not possible to find a simple algorithm which reproduces boundary conditions (4.1) and (4.2). The first term in eq.(A8) determines the kinetic coefficient K_+ . We have chosen the time increment $\Delta t = 1/4N_a$ to set the diffusion coefficient $D_s = 1$. With this choice the kinetic coefficient for the upper terrace is

$$K_+ = 4p_s = \frac{4}{1 + e^{-\phi/k_B T}}. \quad (\text{A9})$$

The coefficient in the second term is smaller than K_+ by a factor $e^{-\phi/k_B T}$, and we suppose that at low temperatures the contribution from the second term is small enough. Similarly

the net number of solidifying atoms from the upper terrace per unit length is approximated in the linear order of the concentration deviation from the equilibrium value as

$$\begin{aligned} \frac{\Delta N_s^- - \Delta N_m^-}{L} &= \frac{(1 - c_{\text{eq}})}{N_a} (c_- - c_{\text{eq}}) (p_s + p_m) \\ &+ \frac{c_{\text{eq}} p_s}{N_a} (c_+ - c_{\text{eq}}). \end{aligned} \quad (\text{A10})$$

The first term yields the kinetic coefficient

$$K_- = 4(1 - c_{\text{eq}}) (p_s + p_m) = \frac{4e^{\phi/k_B T}}{1 + e^{\phi/k_B T}} \left(1 + \frac{1}{1 + e^{\phi/k_B T}} \right), \quad (\text{A11})$$

which is slightly larger than K_+ . The coefficient of the second term is smaller than K_- by a factor $p_s e^{-\phi/k_B T} / (p_s + p_m)$, which is expected to be small at low temperatures. The numbers cited in the paper are calculated with Eqs. (A9) and (A11).

APPENDIX B: WANDERING OF THE PERMEABLE STEP IN GROWTH

1. Isolated step

A step is isolated in an infinitely large facet, and atoms impinge from the vapor with the rate F . When the perturbation $\xi_1 e^{iqx + \omega_q t}$ is given to the straight step, the amplification rate ω_q is calculated as

$$\begin{aligned} \frac{\omega_q x_s^2}{\Omega D_s c_{\text{eq}}^0} &= \frac{-2\Delta\tilde{F}\tilde{v}(\sqrt{\tilde{v}^2 + 4 + 4\tilde{q}^2} - \sqrt{\tilde{v}^2 + 4})}{(2 + \lambda\sqrt{\tilde{v}^2 + 4})(2 + \lambda\sqrt{\tilde{v}^2 + 4 + 4\tilde{q}^2})} \\ &- \frac{2\tilde{\Gamma}\tilde{q}^2\sqrt{\tilde{v}^2 + 4 + 4\tilde{q}^2}}{(2 + \lambda\sqrt{\tilde{v}^2 + 4 + 4\tilde{q}^2})}, \end{aligned} \quad (\text{B1})$$

where $\Delta\tilde{F} = F\tau/c_{\text{eq}}^0 - 1$. For a long-wavelength fluctuation, ω_q is expressed as

$$\omega_q \approx \alpha_2 q^2 - \alpha_4 q^4, \quad (\text{B2})$$

where

$$\alpha_2 = \frac{2[-2\Delta\tilde{F}\tilde{v} - \tilde{\Gamma}(4 + \tilde{v}^2)(2 + \lambda\sqrt{\tilde{v}^2 + 4})]}{\Omega D_s c_{\text{eq}}^0 (2 + \lambda\sqrt{\tilde{v}^2 + 4})^2 \sqrt{\tilde{v}^2 + 4}}, \quad (\text{B3})$$

$$\alpha_4 = -\frac{4[-\Delta\tilde{F}\tilde{v}(2 + 3\lambda\sqrt{\tilde{v}^2 + 4}) + \tilde{\Gamma}(4 + \tilde{v}^2)(2 + \lambda\sqrt{\tilde{v}^2 + 4})]}{\Omega D_s c_{\text{eq}}^0 x_s^2 (1 + \lambda\sqrt{\tilde{v}^2 + 4})^3 (\tilde{v}^2 + 4)^{3/2}}. \quad (\text{B4})$$

If \tilde{v} is small and \tilde{v}^2 is negligible, the amplification rate is given by

$$\frac{\omega_q x_s^2}{\Omega D_s c_{\text{eq}}^0} = \frac{1}{2(1+\lambda)} \left[\frac{-\Delta \tilde{F} \tilde{v}}{(1+\lambda)} - 4\tilde{\Gamma} \right] \tilde{q}^2 - \frac{1}{8(1+\lambda)^2} \left[\frac{-\Delta \tilde{F} \tilde{v}(1+3\lambda)}{(1+\lambda)} + 4\tilde{\Gamma} \right] \tilde{q}^4. \quad (\text{B5})$$

Then critical value of the drift velocity is

$$v_c^W = \frac{4\Omega D_s \tilde{\beta} c_{\text{eq}}^0 (1+\lambda)}{k_B T x_s^2 (c_{\text{eq}}^0 - \tau F)}. \quad (\text{B6})$$

The instability occurs when $\Delta \tilde{F} \tilde{v}$ is negative, i.e., with step-down drift in sublimation and with step-up drift in growth.

2. Steps in a vicinal face

For an equidistant step train with step distance l , the amplification rate ω_q for an in-phase fluctuation is given by

$$\begin{aligned} \frac{\omega_q x_s^2}{\Omega c_{\text{eq}}^0 D_s} = & -\frac{\Delta \tilde{F}}{\lambda g_0} \left(\tilde{v} \sinh \frac{\alpha \tilde{l}}{2} - \alpha \cosh \frac{\alpha \tilde{l}}{2} + \alpha e^{-\tilde{v} \tilde{l}/2} \right) \\ & + \frac{2\Delta \tilde{F}}{\lambda g_0 g_q} \sinh \frac{\alpha_q \tilde{l}}{2} \left(\tilde{v} \sinh \frac{\alpha \tilde{l}}{2} - \alpha \cosh \frac{\alpha \tilde{l}}{2} \right. \\ & \left. + \alpha e^{-\tilde{v} \tilde{l}/2} \right) + \frac{4\alpha v \Delta \tilde{F}}{g_0 g_q} \sinh \frac{\alpha_q \tilde{l}}{2} \\ & \times \left(\cosh \frac{\alpha \tilde{l}}{2} - \cosh \frac{\tilde{v} \tilde{l}}{2} \right) - \frac{2\Delta \tilde{F} \alpha}{g_0 g_q} \\ & \times \left(\cosh \frac{\alpha \tilde{l}}{2} - \cosh \frac{\tilde{v} \tilde{l}}{2} \right) \\ & \times \left(\tilde{v} \sinh \frac{\alpha_q \tilde{l}}{2} + \alpha_q \cosh \frac{\alpha_q \tilde{l}}{2} - \alpha_q e^{-\tilde{v} \tilde{l}/2} \right) \\ & - \frac{\alpha_q}{g_q} \left(\cosh \frac{\alpha_q \tilde{l}}{2} - \cosh \frac{\tilde{v} \tilde{l}}{2} \right) \tilde{\Gamma} \tilde{q}^2. \quad (\text{B7}) \end{aligned}$$

When the step distance is much smaller than the surface diffusion length $l \ll x_s$, and the wavelength of the perturbation is long enough $\tilde{q} = q x_s \ll 1$, ω_q is expanded as

$$\frac{\omega_q}{\Omega D_s c_{\text{eq}}^0} = \left(\frac{-\Delta \tilde{F} \tilde{v} \tilde{l}^5}{360} - \tilde{\Gamma} \tilde{l} \right) \tilde{q}^2 + \dots \quad (\text{B8})$$

The critical drift velocity is given by

$$v_c^W = \frac{360 D_s \Omega \tilde{\beta} c_{\text{eq}}^0 x_s^2}{(c_{\text{eq}}^0 - F \tau) k_B T l^4}. \quad (\text{B9})$$

The instability occurs when $\Delta F v$ is negative, i.e., with step-down drift in sublimation and with step-up drift in growth.

APPENDIX C: WANDERING OF THE IMPERMEABLE STEP IN GROWTH

1. Isolated step

A step is isolated in an infinitely large facet with the impingement of atoms F . The perturbation $\xi_1 e^{iqx + \omega_q t}$ is given to the straight step. The amplification rate ω_q is calculated as

$$\begin{aligned} \frac{\omega_q x_s^2}{\Omega c_{\text{eq}}^0 D_s} = & - \left[\frac{(v-\alpha)(\alpha_q-\alpha)}{[\lambda(v+\alpha_q)+2][\lambda(v+\alpha)+2]} \right. \\ & \left. + \frac{(v+\alpha)(\alpha_q-\alpha)}{[\lambda(v-\alpha_q)-2][\lambda(v-\alpha)-2]} \right] \Delta \tilde{F} \\ & - \left[\frac{(v-\alpha)(\alpha_q-\alpha)}{[\lambda(v+\alpha_q)+2][\lambda(v+\alpha)+2]} \right. \\ & \left. - \frac{(v+\alpha)(\alpha_q-\alpha)}{[\lambda(v-\alpha_q)-2][\lambda(v-\alpha)-2]} \right] \lambda \tilde{F} \tilde{v} \\ & - \frac{\alpha_q + 2\lambda(1+\tilde{q}^2)}{1+\lambda^2(1+\tilde{q}^2)+\alpha\lambda} \tilde{\Gamma} \tilde{q}^2, \quad (\text{C1}) \end{aligned}$$

where $\tilde{F} = F \tau / c_{\text{eq}}^0$. When we take the fast kinetics limit, $\lambda \rightarrow 0$, Eq. (C1) is simplified as

$$\begin{aligned} \frac{\omega_q x_s^2}{\Omega c_{\text{eq}}^0 D_s} = & -\frac{\Delta \tilde{F} \tilde{v}}{2} (\sqrt{\tilde{v}^2 + 4 + 4\tilde{q}^2} - \sqrt{\tilde{v}^2 + 4}) \\ & - \tilde{\Gamma} \tilde{q}^2 \sqrt{\tilde{v}^2 + 4 + 4\tilde{q}^2}, \quad (\text{C2}) \end{aligned}$$

which is the same as Eq. (B1) in the fast kinetics limit. When the step kinetics is slow, $\lambda \gg 1$, the second term in Eq. (C1), proportional to λ^{-1} , is larger than the first term, proportional to λ^{-2} . For the long-wavelength fluctuation, the amplification rate ω_q is given by

$$\frac{\omega_q x_s^2}{\Omega c_{\text{eq}}^0 D_s} \approx \frac{1}{\lambda} (\tilde{F} \tilde{v} - 2\tilde{\Gamma}) \tilde{q}^2 + \dots \quad (\text{C3})$$

Whether in growth or sublimation, with the impingement of atoms, the bunching instability occurs with the step-down drift exceeding the critical value:

$$v_c^W = 2 \frac{\Omega D_s \tilde{\beta} c_{\text{eq}}^0}{\tau F x_s^2 k_B T}. \quad (\text{C4})$$

2. Steps in a vicinal face

For an equidistant train of straight steps, the adatom density is given by

$$c_0(y) = F \tau + c_{\text{eq}}^0 e^{\tilde{v} \tilde{l}/2} \left(A \cosh \frac{\alpha y}{2x_s} + B \sinh \frac{\alpha y}{2x_s} \right), \quad (\text{C5})$$

where l is the step distance, and the coefficients A and B are

$$A = -\frac{\Delta\tilde{F}}{h_0(l)} \left[-\left(\frac{\lambda\tilde{v}}{2} \sinh \frac{\alpha\tilde{l}}{2} - \frac{\lambda\alpha}{2} \cosh \frac{\alpha\tilde{l}}{2} - \sinh \frac{\alpha\tilde{l}}{2} \right) + \frac{\lambda\alpha}{2} e^{-\tilde{v}\tilde{l}/2} \right] \\ + \frac{\tilde{F}\tilde{v}\lambda}{h_0(l)} \left[\left(\frac{\lambda\tilde{v}}{2} \sinh \frac{\alpha\tilde{l}}{2} - \frac{\lambda\alpha}{2} \cosh \frac{\alpha\tilde{l}}{2} - \sinh \frac{\alpha\tilde{l}}{2} \right) + \frac{\lambda\alpha}{2} e^{-\tilde{v}\tilde{l}/2} \right], \quad (\text{C6})$$

$$B = -\frac{\Delta\tilde{F}}{h_0(l)} \left[\left(\frac{\lambda\tilde{v}}{2} \cosh \frac{\alpha\tilde{l}}{2} - \frac{\lambda\alpha}{2} \sinh \frac{\alpha\tilde{l}}{2} - \cosh \frac{\alpha\tilde{l}}{2} \right) \right. \\ \left. + \left(1 + \frac{\lambda\tilde{v}}{2} \right) e^{-\tilde{v}\tilde{l}/2} \right] + \frac{\tilde{F}\tilde{v}\lambda}{h_0(l)} \left[-\left(\frac{\lambda\tilde{v}}{2} \cosh \frac{\alpha\tilde{l}}{2} - \frac{\lambda\alpha}{2} \sinh \frac{\alpha\tilde{l}}{2} - \cosh \frac{\alpha\tilde{l}}{2} \right) + \left(1 + \frac{\lambda\tilde{v}}{2} \right) e^{-\tilde{v}\tilde{l}/2} \right]. \quad (\text{C7})$$

When the step position is perturbed as $\zeta_m = nl + \zeta_l e^{iqx + imkl + \omega_q t}$ by the fluctuation, the amplification rate ω_q is calculated as

$$\frac{\omega_q x_s^2}{\Omega D_s c_{eq}^0} = \frac{u_+}{h_q(l)} \left[-\lambda^2(1 + \tilde{q}^2) \sinh \frac{\alpha_q \tilde{l}}{2} - \frac{\lambda \alpha_q}{2} \cosh \frac{\alpha_q \tilde{l}}{2} - \frac{\lambda \tilde{v}}{2} \sinh \frac{\alpha_q \tilde{l}}{2} + \frac{\lambda \alpha_q}{2} e^{-\tilde{v}\tilde{l}/2} \right] \\ + \frac{u_-}{h_q(l)} \left[-\lambda^2(1 + \tilde{q}^2) \sinh \frac{\alpha_q \tilde{l}}{2} - \frac{\lambda \alpha_q}{2} \cosh \frac{\alpha_q \tilde{l}}{2} + \frac{\lambda \tilde{v}}{2} \sinh \frac{\alpha_q \tilde{l}}{2} + \frac{\lambda \alpha_q}{2} e^{-\tilde{v}\tilde{l}/2} \right] \\ + \frac{1}{h_q(l)} \left[\frac{\lambda \alpha_q u_+}{2} (e^{\tilde{v}\tilde{l}/2} e^{-i\tilde{k}\tilde{l}} - e^{-\tilde{v}\tilde{l}/2}) + \frac{\lambda \alpha_q u_-}{2} (e^{-\tilde{v}\tilde{l}/2} e^{i\tilde{k}\tilde{l}} - e^{-\tilde{v}\tilde{l}/2}) \right] \\ + \frac{\Delta\tilde{F}\lambda}{h_0(l)} \left(\tilde{v} \sinh \frac{\alpha\tilde{l}}{2} - \alpha \sinh \frac{\tilde{v}\tilde{l}}{2} \right) - \frac{\tilde{F}\tilde{v}\lambda}{h_0(l)} \left(\lambda \alpha \cosh \frac{\alpha\tilde{l}}{2} + 2 \sinh \frac{\alpha\tilde{l}}{2} - \lambda \alpha \sinh \frac{\tilde{v}\tilde{l}}{2} \right) \\ - \frac{\Phi(l)}{h_q(l)} \left[2\lambda^2(1 + \tilde{q}^2) \sinh \frac{\alpha_q \tilde{l}}{2} + \lambda \alpha_q \cosh \frac{\alpha_q \tilde{l}}{2} - \lambda \alpha_q \cosh \frac{\tilde{v}\tilde{l} - 2i\tilde{k}\tilde{l}}{2} \right] (1 - \cos \tilde{k}\tilde{l}), \\ - \frac{\tilde{\Gamma}}{h_q(l)} \left[2\lambda^2(1 + \tilde{q}^2) \sinh \frac{\alpha_q \tilde{l}}{2} + \lambda \alpha_q \cosh \frac{\alpha_q \tilde{l}}{2} - \lambda \alpha_q \cosh \frac{\tilde{v}\tilde{l} - 2i\tilde{k}\tilde{l}}{2} \right] \tilde{q}^2, \quad (\text{C8})$$

where

$$u_+ = -\frac{x_s}{\lambda c_{eq}^0} \frac{du_0}{dy} \Big|_{y=0} + \frac{1}{c_{eq}^0} u_0 \Big|_{y=0}, \quad (\text{C9})$$

$$u_- = -\frac{x_s}{\lambda c_{eq}^0} \frac{du_0}{dy} \Big|_{y=l} - \frac{1}{c_{eq}^0} u_0 \Big|_{y=l}, \quad (\text{C10})$$

$$u_0(y) = c_0(y) - F\tau. \quad (\text{C11})$$

We assume that the step distance l is much smaller than the surface diffusion length and all the steps are perturbed with the same phase, i.e., $k=0$. For the slow step kinetics, $l/x_s \ll \lambda$, the amplification rate ω_q is expressed as

$$\frac{\omega_q x_s^2}{\Omega D_s c_{eq}^0} = \tilde{l}(\tilde{v} - \tilde{\Gamma})\tilde{q}^2 + \dots, \quad (\text{C12})$$

which is the same as that in sublimation [Eq. (4.19)]. In the limit of fast kinetics, $\lambda \ll l/x_s$, the amplification rate ω_q is given by

$$\frac{\omega_q x_s^2}{\Omega D_s c_{eq}^0} = \left(-\frac{\Delta\tilde{F}\tilde{v}}{360} \tilde{l}^5 - \tilde{\Gamma}\tilde{l} \right) \tilde{q}^2 + \dots, \quad (\text{C13})$$

which is a generalization of Eq. (3.22). This result coincides with the permeable case [Eq. (B8)], because the gap of the adatom density at the step vanishes in the fast kinetics limit. The instability can occur with the step-down drift in sublimation and with the step-up drift in growth.

APPENDIX D: BUNCHING OF IMPERMEABLE STEPS IN GROWTH

With impingement of adatoms, the velocity of the n th step V_n is given by

$$\begin{aligned}
\frac{2x_s V_n}{\Omega D_s} = & -\lambda \tilde{v} F \tau \frac{(-2\lambda - \tilde{v}) \sinh(\alpha \tilde{l}_+/2) - \alpha \cosh(\alpha \tilde{l}_+/2) - \alpha e^{-\tilde{v} \tilde{l}_+/2}}{(1 + \lambda^2) \sinh(\alpha \tilde{l}_+/2) + \alpha \lambda \cosh(\alpha \tilde{l}_+/2)} \\
& + \lambda \tilde{v} F \tau \frac{(-2\lambda + \tilde{v}) \sinh(\alpha \tilde{l}_-/2) - \alpha \cosh(\alpha \tilde{l}_-/2) - \alpha e^{\tilde{v} \tilde{l}_-/2}}{(1 + \lambda^2) \sinh(\alpha \tilde{l}_-/2) + \alpha \lambda \cosh(\alpha \tilde{l}_-/2)} \\
& - F \tau \frac{(-2\lambda - \tilde{v}) \sinh(\alpha \tilde{l}_+/2) - \alpha \cosh(\alpha \tilde{l}_+/2) + \alpha e^{-\tilde{v} \tilde{l}_+/2}}{(1 + \lambda^2) \sinh(\alpha \tilde{l}_+/2) + \alpha \lambda \cosh(\alpha \tilde{l}_+/2)} \\
& - F \tau \frac{(-2\lambda + \tilde{v}) \sinh(\alpha \tilde{l}_-/2) - \alpha \cosh(\alpha \tilde{l}_-/2) + \alpha e^{\tilde{v} \tilde{l}_-/2}}{(1 + \lambda^2) \sinh(\alpha \tilde{l}_-/2) + \alpha \lambda \cosh(\alpha \tilde{l}_-/2)} \\
& + \frac{[(-2\lambda - \tilde{v}) \sinh(\alpha \tilde{l}_+/2) - \alpha \cosh(\alpha \tilde{l}_+/2) x_s] c_n + \alpha e^{-\tilde{v} \tilde{l}_+/2} c_{n+1}}{(1 + \lambda^2) \sinh(\alpha \tilde{l}_+/2) + \alpha \lambda \cosh(\alpha \tilde{l}_+/2)} \\
& + \frac{[(-2\lambda + \tilde{v}) \sinh(\alpha \tilde{l}_-/2) - \alpha \cosh(\alpha \tilde{l}_-/2)] c_n + \alpha e^{\tilde{v} \tilde{l}_-/2} c_{n-1}}{(1 + \lambda^2) \sinh(\alpha \tilde{l}_-/2) + \alpha \lambda \cosh(\alpha \tilde{l}_-/2)}. \tag{D1}
\end{aligned}$$

The coefficients $\mu_1(l)$ of Eq. (6.4) and $\sigma_1(l)$ of Eq. (6.6) are modified as

$$\mu_1(l) = -2\lambda \tilde{v} \tilde{F} \frac{d}{d\tilde{l}} \left[\frac{2\lambda \sinh(\alpha \tilde{l}/2) + \alpha \cosh(\alpha \tilde{l}/2) + \alpha \cosh(\tilde{v} \tilde{l}/2)}{(1 + \lambda^2) \sinh(\alpha \tilde{l}/2) + \alpha \lambda \cosh(\alpha \tilde{l}/2)} \right] - 2\Delta \tilde{F} \frac{d}{d\tilde{l}} \left[\frac{\tilde{v} \sinh(\alpha \tilde{l}/2) + \alpha \sinh(\tilde{v} \tilde{l}/2)}{(1 + \lambda^2) \sinh(\alpha \tilde{l}/2) + \alpha \lambda \cosh(\alpha \tilde{l}/2)} \right], \tag{D2}$$

$$\sigma_1(l) = \lambda \tilde{v} \tilde{F} \frac{d}{d\tilde{l}} \left[\frac{F \sinh(\alpha \tilde{l}/2) - \alpha \cosh(\tilde{v} \tilde{l}/2)}{(1 + \lambda^2) \sinh(\alpha \tilde{l}/2) + \alpha \lambda \cosh(\alpha \tilde{l}/2)} \right] + \Delta \tilde{F} \frac{d}{d\tilde{l}} \left[\frac{2\lambda \sinh(\alpha \tilde{l}/2) + \alpha \cosh(\alpha \tilde{l}/2) - \alpha \cosh(\tilde{v} \tilde{l}/2)}{(1 + \lambda^2) \sinh(\alpha \tilde{l}/2) + \alpha \lambda \cosh(\alpha \tilde{l}/2)} \right], \tag{D3}$$

where $\tilde{F} = F\tau/c_{\text{eq}}^0$ and $\Delta \tilde{F} = (F\tau/c_{\text{eq}}^0 - 1)$. When the step distance is small, $\alpha l/2x_s \ll 1$, $\mu_1(l)$ becomes

$$\mu_1(l) \approx -4\tilde{v} \frac{d}{d\tilde{l}} \left[\frac{\lambda(\Delta F + 1)(\lambda \tilde{l}/2 + 1) + \Delta F \tilde{l}/2}{(1 + \lambda^2) \tilde{l}/2 + \lambda} \right] = \frac{2\tilde{v} \lambda}{[(\lambda^2 + 1) \tilde{l}/2 + \lambda]^2}, \tag{D4}$$

which is the same as that without impingement [Eq. (6.8)]. Thus, irrespective of the impingement of the adatoms, the vicinal face consisting of impermeable steps can be unstable with the step-down drift.

The derivatives in eq. (D2) are given by

$$\begin{aligned}
\frac{d}{d\tilde{l}} \left[\frac{2\lambda \sinh(\alpha \tilde{l}/2) + \alpha \cosh(\alpha \tilde{l}/2) + \alpha \cosh(\tilde{v} \tilde{l}/2)}{(1 + \lambda^2) \sinh(\alpha \tilde{l}/2) + \alpha \lambda \cosh(\alpha \tilde{l}/2)} \right] = & - \frac{\alpha^2(1 - \lambda^2)}{[(1 + \lambda^2) \sinh(\alpha \tilde{l}/2) + \alpha \lambda \cosh(\alpha \tilde{l}/2)]^2} \\
& - \frac{\alpha(1 + \lambda^2)[\alpha \cosh(\tilde{v} \tilde{l}/2) \cosh(\alpha \tilde{l}/2) - \tilde{v} \sinh(\tilde{v} \tilde{l}/2) \sinh(\alpha \tilde{l}/2)]}{[(1 + \lambda^2) \sinh(\alpha \tilde{l}/2) + \alpha \lambda \cosh(\alpha \tilde{l}/2)]^2} \\
& - \frac{\alpha^2 \lambda [\alpha \cosh(\tilde{v} \tilde{l}/2) \sinh(\alpha \tilde{l}/2) - \tilde{v} \sinh(\tilde{v} \tilde{l}/2) \cosh(\alpha \tilde{l}/2)]}{[(1 + \lambda^2) \sinh(\alpha \tilde{l}/2) + \alpha \lambda \cosh(\alpha \tilde{l}/2)]^2} \tag{D5}
\end{aligned}$$

$$\begin{aligned}
\frac{d}{d\tilde{l}} \left[\frac{\tilde{v} \sinh(\alpha \tilde{l}/2) + \alpha \sinh(\tilde{v} \tilde{l}/2)}{(1 + \lambda^2) \sinh(\alpha \tilde{l}/2) + \alpha \lambda \cosh(\alpha \tilde{l}/2)} \right] = & \frac{\alpha^2 v \lambda}{2[(1 + \lambda^2) \sinh(\alpha \tilde{l}/2) + \alpha \lambda \cosh(\alpha \tilde{l}/2)]^2} \\
& - \frac{\alpha(1 + \lambda^2)[\alpha \sinh(\tilde{v} \tilde{l}/2) \cosh(\alpha \tilde{l}/2) - \tilde{v} \cosh(\tilde{v} \tilde{l}/2) \sinh(\alpha \tilde{l}/2)]}{[(1 + \lambda^2) \sinh(\alpha \tilde{l}/2) + \alpha \lambda \cosh(\alpha \tilde{l}/2)]^2} \\
& - \frac{\alpha^2 \lambda [\alpha \sinh(\tilde{v} \tilde{l}/2) \sinh(\alpha \tilde{l}/2) - \tilde{v} \cosh(\tilde{v} \tilde{l}/2) \cosh(\alpha \tilde{l}/2)]}{[(1 + \lambda^2) \sinh(\alpha \tilde{l}/2) + \alpha \lambda \cosh(\alpha \tilde{l}/2)]^2}. \tag{D6}
\end{aligned}$$

When the step distance is much longer than the surface diffusion length, Eq. (D5) is negative, irrespective of the drift direction. Equation (D6) is negative with the step-down drift and positive with the step-up drift. In sublimation the first

term in Eq. (D2) vanishes, and $-\Delta\tilde{F} = -1$. Then $\mu_1(l)$ is positive, and the vicinal face is unstable with the step-up drift. In growth, $\mu_1(l)$ is positive, and the vicinal face is unstable with the step-down drift.

-
- ¹For a recent review of step dynamics, H.-C. Jeong and E. D. Williams, *Surf. Sci. Rep.* **34**, 171 (1999).
- ²A. V. Latyshev, A. L. Aseev, A. B. Krasilnikov, and S. I. Stenin, *Surf. Sci.* **213**, 157 (1989).
- ³Y. Homma, R. McClelland, and H. Hibino, *Jpn. J. Appl. Phys.* **29**, L2254 (1990).
- ⁴E. D. Williams, E. Fu, Y.-N. Yang, D. Kandel, and D. J. Weeks, *Surf. Sci.* **336**, L746 (1995).
- ⁵Y.-N. Yang, E. S. Fu, and E. D. Williams, *Surf. Sci.* **356**, 101 (1996).
- ⁶H. Yamaguchi and K. Yagi, *Surf. Sci.* **287/288**, 820 (1993).
- ⁷Y. Homma and N. Aizawa, *Phys. Rev. B* **62**, 8323 (2000).
- ⁸D. Kandel and E. Kaxiras, *Phys. Rev. Lett.* **76**, 1114 (1996).
- ⁹S. Stoyanov, *Jpn. J. Appl. Phys.* **30**, 1 (1991).
- ¹⁰A. Natori, *Jpn. J. Appl. Phys.* **33**, 3538 (1994).
- ¹¹C. Misbah, O. Pierre-Louis, and A. Pimpinelli, *Phys. Rev. B* **51**, 17 283 (1995).
- ¹²S. Stoyanov, *Surf. Sci.* **416**, 200 (1998).
- ¹³J. J. Métois and S. Stoyanov, *Surf. Sci.* **440**, 407 (1999).
- ¹⁴B. Houchmandzadeh, C. Misbah, and A. Pimpinelli, *J. Phys. I* **4**, 1843 (1994).
- ¹⁵C. Misbah and O. Pierre-Louis, *Phys. Rev. E* **53**, R4319 (1996).
- ¹⁶M. Sato and M. Uwaha, *J. Phys. Soc. Jpn.* **65**, 1515 (1996).
- ¹⁷D.-J. Liu, D. J. Weeks, and D. Kandel, *Surf. Rev. Lett.* **4**, 107 (1997).
- ¹⁸D.-J. Liu and D. J. Weeks, *Phys. Rev. B* **57**, 14 891 (1998).
- ¹⁹S. Stoyanov and V. Tonchev, *Phys. Rev. B* **58**, 1590 (1998).
- ²⁰M. Sato and M. Uwaha, *J. Phys. Soc. Jpn.* **47**, 3675 (1998).
- ²¹M. Sato and M. Uwaha, *Surf. Sci.* **442**, 318 (1999).
- ²²M. Sato and M. Uwaha, *Phys. Rev. E* **60**, 7120 (1999).
- ²³M. Degawa, H. Minoda, Y. Tanishiro, and K. Yagi, *Surf. Sci.* **461**, L528 (2000).
- ²⁴M. Sato and M. Uwaha, *J. Phys. Soc. Jpn.* **65**, 2146 (1996).
- ²⁵M. Sato, M. Uwaha, and Y. Saito, *Phys. Rev. Lett.* **80**, 4233 (1998).
- ²⁶M. Degawa, H. Nishimura, Y. Tanishiro, H. Minoda, and K. Yagi, *Jpn. J. Appl. Phys.* **38**, L308 (1999).
- ²⁷K. Fujita, M. Ichikawa, and S. Stoyanov, *Phys. Rev. B* **60**, 16 006 (1999).
- ²⁸M. Ozdemir and A. Zangwill, *Phys. Rev. B* **45**, 3718 (1992).
- ²⁹M. Uwaha and P. Nogières, in *Morphology and Growth Unit of Crystals*, edited by I. Sunagawa (Terra Scientific, Tokyo, 1989), p. 17.
- ³⁰V. I. Marchenko and A. Ya. Parshin, *Zh. Eksp. Teor. Fiz.* **79**, 257 (1980) [*Sov. Phys. JETP* **52**, 129 (1980)].
- ³¹M. Uwaha and Y. Saito, *Phys. Rev. Lett.* **68**, 224 (1992).
- ³²Y. Saito and M. Uwaha, *Phys. Rev. B* **49**, 10 677 (1994).
- ³³In Ref. 25, although the dispersion is calculated for an impermeable step with the fast kinetics limit, we used the same algorithm as that used here. As shown in Sec. IV, the wandering behavior is similar for impermeable steps. If we use Eq. (3.5) for the estimation of λ_{\max} , the agreement with the simulation [Fig. 2(c) in Ref. 25)] is improved.
- ³⁴W. K. Burton, N. Cabrera, and F. C. Frank, *Philos. Trans. R. Soc. London* **243**, 299 (1951).
- ³⁵A. Karma and C. Misbah, *Phys. Rev. Lett.* **71**, 3810 (1993).
- ³⁶Y. Kuramoto, *Prog. Theor. Phys.* **71**, 1182 (1984).
- ³⁷Y. Kuramoto and T. Tsuzuki, *Prog. Theor. Phys.* **55**, 356 (1976).
- ³⁸G. I. Sivashinsky, *Acta Astronaut.* **4**, 1177 (1977).
- ³⁹I. Bena, C. Misbah, and A. Valance, *Phys. Rev. B* **47**, 7408 (1993).
- ⁴⁰Y. Saito and M. Uwaha, *J. Phys. Soc. Jpn.* **65**, 3576 (1996).
- ⁴¹M. Sato and M. Uwaha, *J. Cryst. Growth* **198/199**, 38 (1999).
- ⁴²M. Uwaha and M. Sato, *Surf. Rev. Lett.* **5**, 841 (1998).
- ⁴³G. Ehrlich and F. G. Hudda, *J. Chem. Phys.* **44**, 1039 (1966).
- ⁴⁴R. L. Schwoebel and E. J. Shipsey, *J. Appl. Phys.* **37**, 3682 (1966).
- ⁴⁵G. S. Bales and A. Zangwill, *Phys. Rev. B* **41**, 5500 (1990).
- ⁴⁶A. Pimpinelli, I. Elkinani, A. Karma, C. Misbah, and J. Villain, *J. Phys.: Condens. Matter* **6**, 2661 (1994).
- ⁴⁷M. Sato and M. Uwaha, *Phys. Rev. B* **51**, 11 172 (1995).
- ⁴⁸M. Sato and M. Uwaha, *Europhys. Lett.* **38**, 639 (1995).
- ⁴⁹M. Uwaha, *J. Phys. Soc. Jpn.* **57**, 1681 (1988).
- ⁵⁰W. W. Mullins, in *Metal Surfaces*, edited by W. D. Robertson and N. A. Gjostein (Metall. Soc. AIME, Metals Park, OH, 1963).
- ⁵¹M. Uwaha, *Phys. Rev. B* **46**, 4364 (1992).
- ⁵²M. Uwaha, *J. Cryst. Growth* **128**, 92 (1993).